



Use of Landsat thermal imagery in monitoring evapotranspiration and managing water resources

Martha C. Anderson ^{a,*}, Richard G. Allen ^b, Anthony Morse ^c, William P. Kustas ^a

^a USDA-ARS, Hydrology and Remote Sensing Lab, Bldg. 007, BARC West, Beltsville, MD 20705, United States

^b University of Idaho, Kimberly Research and Extension Center, Kimberly, ID 83301, United States

^c Spatial Analysis Group, Boise, ID 83701, United States

ARTICLE INFO

Article history:

Received 16 March 2011

Received in revised form 27 July 2011

Accepted 28 August 2011

Available online 16 February 2012

Keywords:

Evapotranspiration

Thermal remote sensing

Landsat

Water resource management

Drought

ABSTRACT

Freshwater resources are becoming increasingly limited in many parts of the world, and decision makers are demanding new tools for monitoring water availability and rates of consumption. Remotely sensed thermal-infrared imagery collected by Landsat provides estimates of land-surface temperature that allow mapping of evapotranspiration (ET) at the spatial scales at which water is being used. This paper explores the utility of moderate-resolution thermal satellite imagery in water resource management. General modeling techniques for using land-surface temperature in mapping the surface energy balance are described, including methods developed to safeguard ET estimates from expected errors in the remote sensing inputs. Examples are provided of how remotely sensed maps of ET derived from Landsat thermal imagery are being used operationally by water managers today: in monitoring water rights, negotiating interstate compacts, estimating water-use by invasive species, and in determining allocations for agriculture, urban use, and endangered species protection. Other applications include monitoring drought and food insecurity, and evaluation of large-scale land-surface and climate models. To better address user requirements for high-resolution, time-continuous ET data, novel techniques have been developed to improve the spatial resolution of Landsat thermal-band imagery and temporal resolution between Landsat overpasses by fusing information from other wavebands and satellites. Finally, a strategy for future modification to the Landsat program is suggested, improving our ability to track changes in water use due to changing climate and growing population. The long archive of global, moderate resolution TIR imagery collected by the Landsat series is unmatched by any other satellite program, and will continue to be an invaluable asset to better management of our earth's water resources.

Published by Elsevier Inc.

1. Introduction

Land-surface evapotranspiration (ET) transfers large volumes of water (and energy, in the form of latent heat) from the soil (evaporation) and vegetation (transpiration) into the atmosphere. Accurate, spatially distributed information on water use, quantified at the scale of human influence, has been a long-standing critical need for a wide range of applications. Quantifying ET from irrigated crops is vital to management of water resources in areas of water scarcity, and detailed maps enable managers to more judiciously allocate available water among agricultural, urban, and environmental uses. The actual rate of water use by vegetation can deviate significantly from potential ET rates (as regulated by atmospheric demand for water vapor) due to impacts of drought, disease, insects, vegetation amount and phenology, and soil texture, fertility and salinity. Satellite-derived indices reflecting the difference between actual and potential ET are used globally to

identify crop water deficits and causes of low food production, and form a major component of our national food security program. Diagnostic estimates of ET can be used to infer soil moisture conditions – a valuable input to weather, drought, and flood forecast models, and critical to many military applications. On still larger scales, spatial patterns in ET play an essential role in mesoscale and general circulation modeling, affecting cycling of water and energy between the land, oceans and atmosphere.

Dwindling supplies of fresh water are a problem worldwide, and demand for more spatially detailed quantification of ET is growing as demands on water resources come under increasing competition. The U.S. Department of the Interior predicts significant water shortages throughout the American West resulting from limited supply coupled with explosive population growth. Climate change research suggests this scenario will be echoed around the globe, striking most severely the arid and semiarid regions that have the least buffer in terms of stored water supply. The Strategic Plan for the U.S. Integrated Earth Observation System has identified “*Protection and Monitoring of Water Resources*” as one of nine application focus areas for earth observation for *Societal Benefit*. Already, satellite-based ET

* Corresponding author at: Bldg 007, Rm 104 BARC-West, 10300 Baltimore Ave, Beltsville, MD 20705, United States. Tel.: +1 301 504 6616; fax: +1 301 505 8931.

E-mail address: martha.anderson@ars.usda.gov (M.C. Anderson).

mapping has been integrated into operational water management programs within the US. Remotely sensed ET has been used to develop water budgets, to monitor aquifer depletion, to understand water use change with land use, to optimize irrigation to protect endangered species habitat, to monitor water rights compliance, and to estimate agricultural water use for water-right buy-back programs for mitigation and litigation. Based on these successful implementations, the Western States Water Council (WSWC) has voiced strong support for continued nation-wide water data collection using satellite remote sensing (www.westgov.org/wswc/-325 nasa position 29oct 2010.pdf; landsat.gsfc.nasa.gov/news/news-archive/soc_0023.html).

To address these growing needs for ET data, land-surface temperature (LST) maps, derived from thermal infrared (TIR) imagery collected by satellites and aircraft, have proven to be a valuable asset in mapping ET over large areas. The LST state variable is highly sensitive to local moisture conditions and effects of evaporative cooling, and plays a key role in diagnosing many of the major surface energy balance components, including sensible heat, net radiation, and soil heat flux. For management and monitoring, the TIR band has an advantage over the soil-moisture sensitive microwave band in that TIR can be used to retrieve moisture information at several orders of magnitude higher spatial resolution. Several TIR-based approaches to mapping ET have been developed in support of water resource applications, using LST as the primary input (e.g., Allen et al., 2007a; Bastiaanssen et al., 1998; Su, 2002). The most successful of these incorporate novel strategies to reduce sensitivity to expected errors in LST retrieval due to atmospheric and emissivity corrections to TIR imagery.

In this paper, we describe some of these approaches, and demonstrate the unique value of LST data and ET mapping at the ~100-m scale, which we define as “moderate resolution” to distinguish from the high-resolution (meter scale) shortwave imagery collected by many commercial satellites. The 100-m resolution characteristic of TIR imagery collected by the Landsat series of satellites has proven critical to many operational needs for ET data because it will typically enable discrimination of individual agricultural fields and major waterways – landscape features that are blurred or completely unresolved at the coarser 1-km TIR resolution of instruments like the Moderate resolution Imaging Spectrometer (MODIS) and the Advanced Very High Resolution Radiometer (AVHRR), or the 25-km + resolution of microwave-based soil moisture retrievals. These various moisture-related data streams can be combined to improve spatio-temporal coverage, but the sub-field scale surface temperature information provided by Landsat is essential for connecting TIR signals sensed at the satellite with recognizable features on the landscape. In addition, the long period of record associated with the Landsat TIR archive (back to the launch of Landsat 4 in 1982) allows us to track changes in water consumption by specific users over time – a necessity for legal applications such as monitoring water rights compliance and negotiating interstate water compacts, or for studying the response of water use patterns under changing climatic and land-use conditions.

A comprehensive global water resource monitoring program will utilize satellite information at multiple scales and wavelengths: merging optical, TIR, and microwave data from polar and geostationary platforms. Here we focus on value added to existing regional monitoring tools by TIR data collected by Landsat at the scale of human intervention in the natural water cycle.

2. The specific need for moderate resolution thermal imagery

Water consumption by crops is by far the largest use of freshwater resources on earth. Globally, 1.5 billion ha of cropland (irrigated and rainfed) cover about 10% of the earth's terrestrial surface (Thenkabail et al., 2009). About 80% of freshwater consumption by humans is used for irrigated agriculture that produces 45% of the total world

food supply from 25% of the world's croplands (399 million ha) (Thenkabail et al., 2010). Water consumption from irrigated agriculture is estimated to total about 1200 km³ per year of abstracted water in addition to 920 km³ per year of incident rainfall (Thenkabail et al., 2010). Total water consumption by all agricultural vegetation, both irrigated and rainfed, is estimated to be 6700 km³ per year (6.7 trillion m³).

Rates of water consumption are governed by a combination of surface energy availability (weather and climate), soil water availability (precipitation, irrigation, and shallow water tables), and the amount, type and health of the vegetation. Plant water use is regulated by stomatal aperture, and studies at the leaf, plant and canopy scale have demonstrated the utility of TIR measurements for assessing plant water relations (Jones et al., 2002), canopy/stomatal conductance (Blonquist et al., 2009; Jones and Leinonen, 2003; Leinonen et al., 2006), and monitoring stomatal closure (Jones and Leinonen, 2003). These biophysical properties regulate transpiration rates and can be highly variable, both spatially and temporally. Evaporation of water from exposed soil surfaces also has a thermal signature, and can lead to small-scale structure in landscape ET. In agricultural and heterogeneous natural systems, significant variability in ET and LST can occur at scales of hundreds of meters or less.

Moderate-resolution satellite TIR imagery is therefore required to identify the water consumption associated with specific crop types and land holdings, and to provide information relevant to food producers. This resolution is also needed to study variability in water consumption within individual fields and plant communities for the purposes of improving water-use efficiency of crops, and for identifying particularly water-inefficient (often invasive) species. A typical irrigated field in the western US, for example, has dimensions of 800 × 800 m or less. With the 60-m thermal pixel size of Landsat 7, up to 100 thermal pixels will be completely contained within an 800 × 800 m field (after buffering in from edges). With Landsat 5, at 120 m in the TIR band, one can discern 15 to 20 thermal pixels within a single field. This kind of sampling provides valuable information regarding spatial variability of ET within fields and uniformity of water consumption. Multiple within-field samples also improve the accuracy of estimated total water consumption associated with an individual field. However, farm and field sizes in many regions of the world are significantly smaller, especially in developing countries where fields may be even less than 0.1 ha (30 m × 30 m). A reasonable future target for monitoring by satellite may be 1 ha fields (100 × 100 m), arguing for a resolution of 20 to 30 m on next-generation TIR sensors.

Low-resolution satellites (thermal pixel size ≥ 1 km on a side) are useful for developing regional, continental or global scale water budget assessments. However, these products do not provide the necessary spatial detail required to meet water and biomass monitoring needs for practical management. Although the MODIS instruments (first launched in 1999) have a daily return time (one overpass per day at varying view angles), their effective thermal resolution is 1000–2000 m depending on sensor view angle, prohibiting assessment of water consumption by individual crops and fields. An average-sized center pivot (typically 800 m in the US) will be embedded within a single thermal pixel, or worse yet, split between two MODIS thermal pixels, and specific thermal information for the individual field is lost (Fig. 1).

A similar issue arises in river management. The US Bureau of Reclamation (USBR) requires accurate information regarding evaporative water losses along major waterways to plan water releases to support mandated downstream flows. As demonstrated in Fig. 2, MODIS TIR is unable to resolve water loss from the narrow riparian mesquite canopy along the highlighted stretch of the San Pedro River in Arizona, and therefore does not produce useful information for decision making (Li et al., 2008). The need to resolve small hydrologic features important to basin-scale management, such as small reservoirs and irrigation canals, also argues for a higher future TIR resolution of 20–30 m.

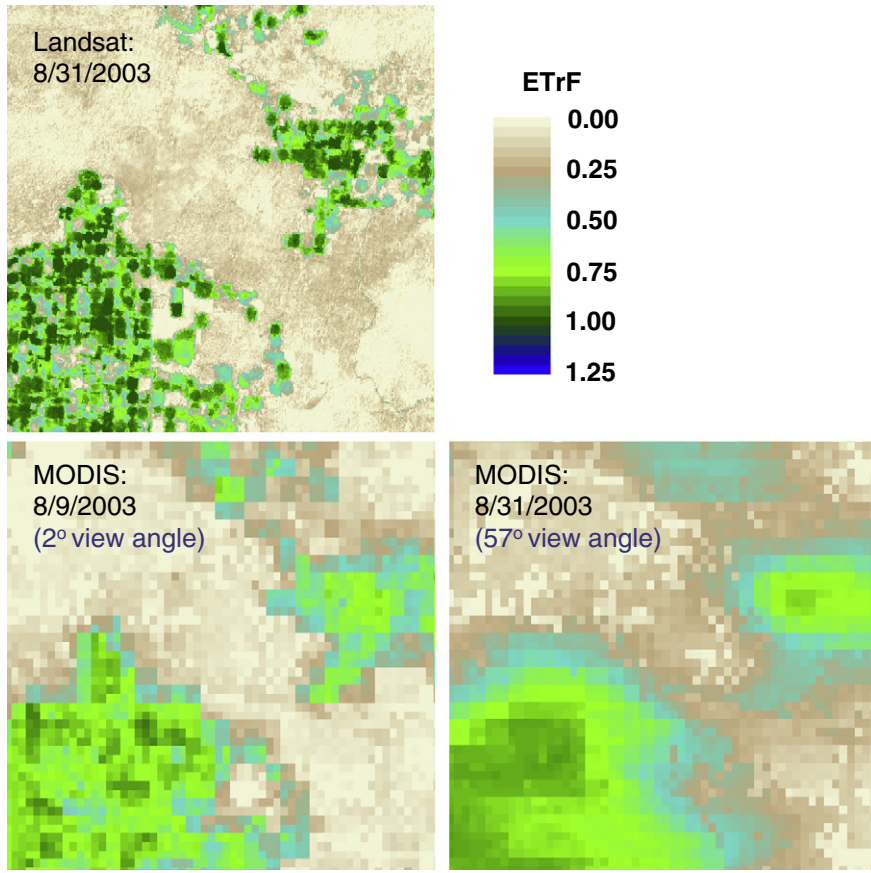


Fig. 1. Ratios (ETrF) of actual ET to 'reference' ET represented by full-cover alfalfa for a 25 × 25 km area of desert and irrigated agriculture in southern Idaho, derived from Landsat (top) and MODIS (bottom left and right) imagery using METRIC. MODIS imagery on the same date as the Landsat image had a 57° view angle, which substantially decreases the effective resolution of the retrieved ET. A typical center pivot size is 800 m in diameter (quarter section, or half mile × half mile).

While the coarse scale of MODIS is valuable for landscape and river basin-scale ET retrievals, and the daily revisit time can be useful for following time-variable changes in ET, it is clear that the nominal 100-m resolution of Landsat is essential for applications where a thermal satellite signal must be unequivocally associated with a specific activity, process, or land-surface feature on the ground, such as in managing irrigation water rights and monitoring water consumption along narrow riparian ecosystems.

3. TIR-based approaches to mapping ET

Over the past few decades, models using TIR-derived measurements of land-surface radiometric temperature (T_{RAD}) to constrain spatially distributed estimates of ET have become increasingly sophisticated. Gradient-resistance flux models provide a micrometeorologically based representation of the surface energy balance, typically treating the land-surface within the TIR pixel as a single homogeneous source of flux and radiometric emission (single or blended source), or evaluating contributions from the soil and canopy components of the scene independently (dual source). Thermal gradient-resistance models generally estimate evapotranspiration (or latent heat flux, when expressed in units of energy) by partitioning the energy available at the land surface ($RN - G$, where RN is net radiation and G is the soil heat conduction flux) into turbulent fluxes of sensible and latent heating (H and λE , respectively):

$$RN - G = H + \lambda E. \quad (1)$$

In classical approaches, the TIR data are used to compute H from the aerodynamic temperature, T_{AERO} (related to the surface

radiometric temperature, T_{RAD}) and an above-canopy air temperature, T_{AIR} :

$$H = \rho c_p \frac{T_{AERO} - T_{AIR}}{R_A} \quad (2)$$

where ρc_p is the heat capacity of air, and R_A is the aerodynamic resistance to turbulent transport between the heights above ground level associated with the quantities T_{AERO} and T_{AIR} and depends on local wind speed, surface roughness and stability in the atmospheric surface layer. The available energy, $RN - G$, is modeled from estimates of downwelling and upwelling radiation and canopy radiative transfer, then λE (or some portion thereof) is derived as a residual to Eq. (1).

There are several practical issues related to the computation of H using Eq. (2). The aerodynamic temperature is a theoretical construct, effectively defined such that Eq. (2) holds (Norman and Becker, 1995), but is not directly measurable. T_{AERO} is related to T_{RAD} , but not identical and can differ by several degrees. The relationship depends on several factors including TIR sensor view angle, vegetation cover fraction, and the surface roughness length for heat and momentum. Another major challenge lies in accurately specifying the required meteorological boundary conditions in T_{AIR} (Eq. 1). Feedback between the surface and atmosphere can cause local T_{AIR} to be very different (by several degrees) from shelter-level conditions at the nearest synoptic weather station, having typical spacing in the U.S. of 100 km. Given that standard meteorological data are typically collected at airports over grass or bare soil surfaces, interpolation of T_{AIR} to any specific location (pixel) having different energy partitioning conditions, such as desert rangeland or irrigated agriculture, for example, can cause large errors in the assumed vertical temperature gradient and resulting flux

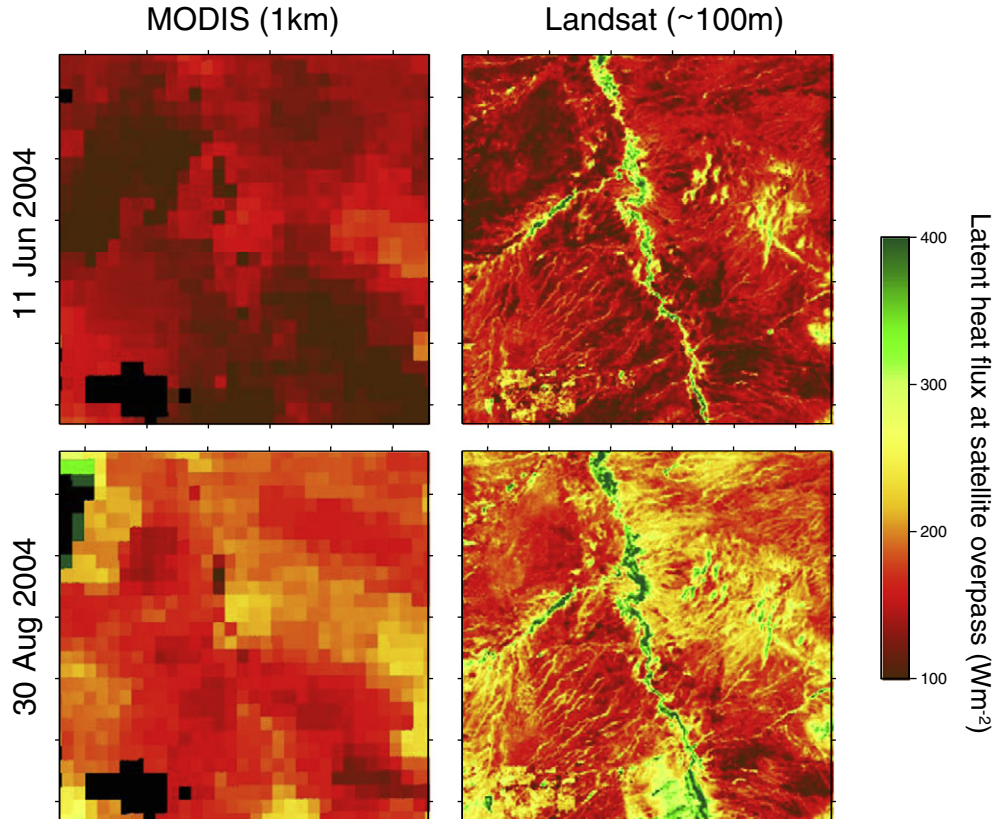


Fig. 2. Latent heat flux maps generated with DisALEXI at the time of satellite overpass using TIR imagery from MODIS (left) and Landsat (right) on 11 June (top) and 30 August 2004 (bottom). Boxes are 30×30 km and cover a stretch of the San Pedro River outside of Tombstone, AZ. The MODIS LST products used in the DisALEXI algorithm show no significant signal over the riparian channel, and therefore the associated evaporative water loss is not accounted for at this scale.

estimates. These errors are further exacerbated by inevitable biases in T_{RAD} due to inaccurate sensor calibration and atmospheric and emissivity corrections, which will further corrupt estimation of $T_{AERO} - T_{AIR}$ (Anderson et al., 1997; Norman et al., 1995a).

Problems encountered in applying Eq. (2) directly led to early skepticism regarding the utility of TIR in ET mapping (Hall et al., 1992) — a bias that still lingers today (Cleugh et al., 2007; Mu et al., 2007, 2011). This skepticism contributed to initial plans for eliminating thermal imaging capacity on the upcoming Landsat Data Continuity Mission — a decision that was later reversed (Irons et al., 2012—this issue). However, more recent studies have demonstrated that TIR data can be effectively integrated into energy balance modeling if care is taken to minimize impacts of expected observational errors in T_{RAD} and T_{AIR} and to properly represent the land-atmosphere exchange and radiometric emission from a heterogeneous land surface (Kalma et al., 2008). Two representative classes of TIR modeling approaches designed for operational applications are discussed here.

3.1. TIR contextual scaling approach (SEBAL/METRIC)

This general technique was pioneered by Price (1990) and uses contextual information from within the satellite image to scale between TIR end-member pixels representing non-limiting moisture availability (potential ET; cold pixel) and zero or limited extractable moisture (little or no ET; hot pixel). In this way, the need for absolute accuracy in the TIR imagery is reduced, as long as relative variability in LST is captured with good fidelity.

The Surface Energy Balance Algorithm for Land (SEBAL; Bastiaanssen et al., 1998) uses a single-source, blended gradient-resistance approach, but replacing $T_{AERO} - T_{AIR}$ in Eq. (2) with a near-surface gradient ΔT that

is determined through scaling rather than through direct estimation or measurement of either T_{AERO} or T_{AIR} . ΔT is determined from Eq. (2) at two extreme (wet and dry) conditions within the scene by inverse modeling of the energy balance ($H = \lambda E - RN - G$), assuming λE is near potential and near zero at these extremes. The SEBAL approach assumes that ΔT scales linearly with T_{RAD} across the imaging scene between the two end-member conditions, an assumption that appears to hold over a range of land use types and aerodynamic roughness conditions (Bastiaanssen et al., 2005). Then H is retrieved at each pixel based on the scene-calibrated linear ΔT vs. T_{RAD} equation and λE is computed by residual. The intention of the approach is to embed residual errors in modeled RN , G and surface aerodynamic properties preferentially into the internally calibrated H component, leaving a more reliable estimate of λE , which is constrained to lie between physically realistic bounds.

The Mapping Evapotranspiration with Internalized Calibration (METRIC; Allen et al., 2007b) algorithm evolved from SEBAL, but uses ground-based micrometeorological measurements of reference ET acquired within the scene to establish the latent heat flux at the cold pixel, rather than assuming *a priori* that $H = 0$ for that condition. Because of the robustness imparted by the internal calibration mechanism, both of these algorithms have been used extensively in water management applications, with minimal reliance on ancillary information (Allen et al., 2007a; Bastiaanssen et al., 2000).

A practical limitation of contextual scaling approaches like SEBAL and METRIC is that they assume that the endpoint conditions are present in every scene (large contrast) and can be accurately identified or can be adequately modeled (e.g., using a residual evaporation model at the dry end; Allen et al., 2007b). These approaches generally require subjective user intervention by trained modelers to select appropriate endpoint pixels, or development of an automated selection algorithm.

The endpoints are best defined in high resolution imagery, with small, homogeneous pixels – application can be more challenging with coarser instruments like AVHRR or MODIS (Allen et al., 2007b; Carlson, 2007; Price, 1990). Such approaches may be difficult to apply over continental and even regional scales, where scaling can become significantly non-linear and multi-valued due to large variations in radiative forcing, topography, sensor view angle, and air mass and landcover conditions (Timmermans et al., 2007).

Bastiaanssen et al. (2005) reported errors in SEBAL applications over a broad range of soil wetness and plant community conditions to average about 15% at the field scale when applied to an individual satellite image date, improving to 5% for ET integrated to a seasonal basis. He suggested the accuracy of annual ET over large watersheds may be similar, if the process is applied by experienced users. Allen et al. (2007b) compared ET estimation by METRIC with measurements by precision weighing lysimeters for agricultural crops and found mean absolute differences of 14% on Landsat image dates during the crop growing periods. Standard deviation of differences over the time periods represented by each satellite image averaged 20% including dormant periods and 13% during the growing period. In a second comparison for irrigated grass hay, monthly ET derived from Landsat images averaged $+/- 16\%$ relative to lysimeter measurements. However, when monthly ET was summed to growing season totals, in each case, error was reduced to less than 5% over the growing period due to reduction in random errors due, for example, to incidences of surface wetting by irrigation or precipitation prior to or between imaging scenes and other modeling errors.

3.2. TIR time-differencing approach (ALEXI/DisALEXI)

Another scheme for improving robustness in thermal-derived ET estimates is to use a time-differential (as opposed to absolute) temperature signal, relating diurnal or morning LST changes to surface moisture availability and latent heat flux (Carlson, 1986; Price, 1980; Wetzel et al., 1984). Differential TIR measurements are less sensitive to errors in sensor calibration, and atmospheric /emissivity corrections than are absolute temperature data. Development of “thermal inertia” models of ET were inspired by the launch of the Heat Capacity Mapping Mission in 1978, providing TIR observations at 2 AM and 2 PM at 500-m spatial resolution, and subsequently adapted for geostationary data (Diak and Stewart, 1989; Wetzel et al., 1984). The underlying physical principle is that soil

moisture increases heat capacity and evaporative cooling of the land surface, thereby reducing the amplitude of the diurnal temperature wave.

Norman et al. (1995b) demonstrated that T_{AERO} can be reliably yet parsimoniously related to T_{RAD} if fluxes from the soil and canopy components of the TIR imaging scene are considered separately, forming a two-source energy balance (TSEB) modeling framework. The TSEB has been demonstrated to work well at point scale over a wide range in cover and climatic conditions and TIR sensor viewing angles, using only a modicum of ancillary data (Anderson et al., 2008; Kustas and Norman, 1999, 2000; Kustas et al., 1995; Li et al., 2005; Zhan et al., 1996). In the regional Atmosphere-Land Exchange Inverse (ALEXI; Anderson et al., 1997, 2007c) model, the TSEB is applied at two times during the morning atmospheric boundary layer (ABL) growth phase using radiometric temperature data from a geostationary platform. Energy closure over this interval is provided by a simple slab model of ABL development (McNaughton and Spriggs, 1986), relating the rise in air temperature in the mixed layer to the time-integrated influx of sensible heat from the land surface. This coupling eliminates the need for *a priori* specification of T_{AIR} ; rather, near-surface air temperature is computed internally at the interface between the surface and ABL model components. Due to its time-differential nature, ALEXI uses only the time change signal in T_{RAD} over the morning interval and the early morning atmospheric lapse rate above ~ 50 –100 m (obtained from mesoscale analyses of synoptic radiosonde observations), greatly reducing sensitivity to errors in absolute temperature retrieval (Anderson et al., 1997).

Because this approach requires no subjective user interaction, the modeling system can be fully automated. ALEXI currently runs daily in near real-time on a 10-km grid covering the continental US using data from the GOES-E and W satellites (Anderson et al., 2007c), and a global product is under development using the international constellation of geostationary satellites (Anderson et al., 2011b). While ALEXI is constrained to run at the coarser scales of geostationary TIR imagery (3–10 km), an associated spatial disaggregation technique (DisALEXI; Norman et al., 2003) can be used to produce higher resolution flux maps at 10^0 – 10^3 meter resolution using images from polar orbiting satellite sensors like Landsat and MODIS, facilitating consistent flux evaluations at local to continental scales (Anderson et al., 2007b).

A limitation of the DisALEXI approach is that generation of the ALEXI boundary conditions can be cumbersome in initial set-up, requiring mesoscale analyses of ABL profiles and collection of hourly geostationary data. To facilitate localized applications of the TSEB in high-resolution

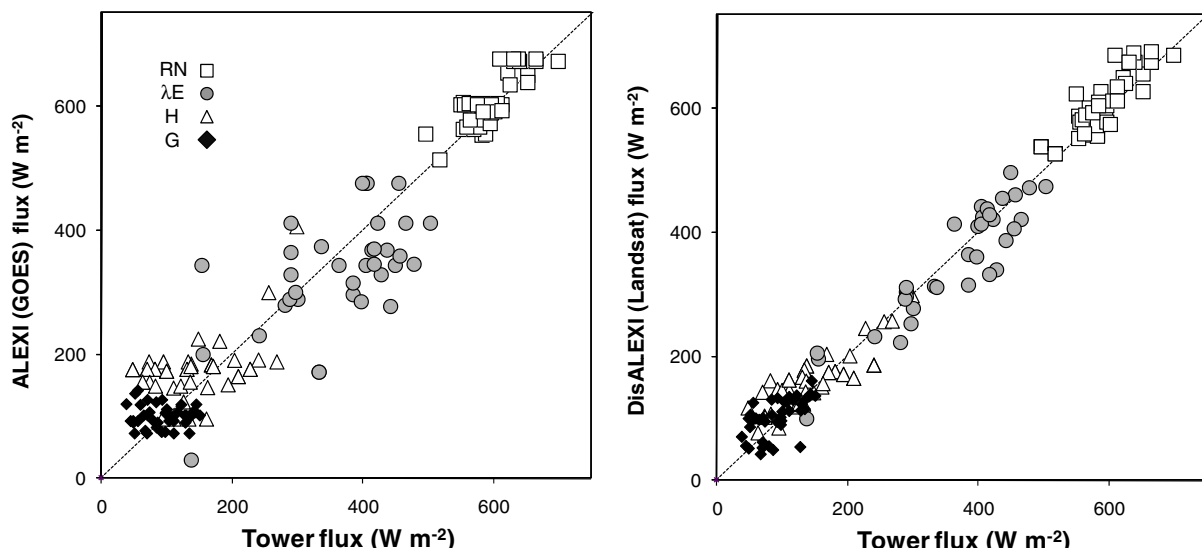


Fig. 3. Comparison of instantaneous flux estimates from ALEXI (using GOES-5 km TIR) and DisALEXI (using Landsat 60-m TIR) at the time of the Landsat overpass with eddy covariance flux tower observations collected during field campaigns in central Iowa and in Oklahoma, and measurements from the Oklahoma Mesonet.

mapping mode without the need for ALEXI, [Cammalleri et al. \(in review\)](#) have proposed a hybrid approach, integrating the concept of end-member ET specification used in SEBAL/METRIC. The Dual Temperature Difference model is a simplified version of ALEXI, using an observed or analyzed air temperature change field as input in place of the ABL component ([Kustas et al., 2001; Norman et al., 2000](#)).

Landsat TIR allows model evaluation at the scale of the flux observation footprint, typically <100 m in the case of short flux towers, and therefore provides more realistic accuracy assessments. [Fig. 3](#) summarizes model evaluation experiments with respect to observations from tower networks in Oklahoma and central Iowa ([Anderson et al., 2007b](#)), showing mean absolute differences of 9% with respect to half-hourly eddy covariance (EC) measurements of latent heat flux at the Landsat overpass time (right panel). Comparing 5-km GOES-derived fluxes directly to the tower fluxes yields 19% errors in latent heat (left panel). At this scale, model-related errors are confounded by errors in representativity of a 100-m observation within a 5-km patch of heterogeneous landscape, providing only an upper limit on the actual model errors. Disaggregated fluxes have also been compared with EC flux measurements collected by aircraft in Iowa and Oklahoma, demonstrating the model reproduced both magnitude and spatial variability in ET over the transects ([Anderson et al., 2005; Anderson et al., 2008; Kustas et al., 2006](#)). A comprehensive evaluation of ALEXI/DisALEXI using EC observations from international Fluxnet sites over a range in cover types and climatic conditions is underway.

3.3. Mapping ET without LST

Remote sensing approaches have also been developed for mapping ET without using TIR data as input. The most widely used of these is the crop coefficient approach, where a reference ET (ET_r , the non-water limited ET from a reference surface, typically short-clipped grass or alfalfa) determined from meteorological data is modified by satellite-derived coefficients (K_c) reflecting the typical water-use of specific crops or natural (unmanaged) vegetation:

$$ET = K_c * ET_r. \quad (3)$$

([Allen et al., 1998](#)). An alternative dual crop coefficient formulation represents K_c as a sum of coefficients representing the transpiration (K_{cb}) and soil evaporation (K_e) components of ET, where K_e is determined using precipitation and simulated irrigation data in a soil water balance model ([Allen et al., 1998](#)). These models have been found to work well in assessing the crop water requirements of a variety of irrigated crops ([Hunsaker, 1999; Hunsaker et al., 2003; Tolk and Howell, 2001](#)). For larger area assessments, shortwave vegetation indices (VIs) such as the Normalized Difference Vegetation Index (NDVI) relating reflectances in the red and near infrared bands have been successfully used to map K_c over agricultural landscapes to provide information on when to apply irrigation ([Bausch, 1995; Bausch and Neale, 1987, 1989; Hunsaker et al., 2003](#)), and over natural riparian landscapes to describe water-use by invasive species (e.g., [Nagler et al., 2005](#)). The K_c -VI relationship must be derived empirically for each crop/vegetation type using local ET measurements.

These VI approaches to ET mapping can produce usable estimates under certain conditions and have some practical advantages over TIR-based energy balance models: 1) VI data can be easily derived at relatively high resolution from a number of existing shortwave satellite systems; 2) VIs change relatively slowly in comparison with surface moisture conditions reflected in the LST, and therefore sampling frequency may be less of an issue (although slow response to moisture conditions can also be a detriment to VI methods; see below); and 3) VI methods are typically easier to code and simpler to implement than energy balance algorithms. VI methods tend to work best in irrigated and riparian areas that are perennially unstressed, or over longer timescales where vegetation indices have

time adjust to local moisture conditions. They have good skill in estimating water use requirements by managed crops – i.e., how much water must be used to keep the crop in reasonable health.

VI approaches are less well-suited for routine satellite monitoring of *actual* water use over generalized landscapes, or for detecting onset of stress conditions in natural and agricultural ecosystems. It is often these applications, where VI and ET are *not* well correlated, that are of most interest. Furthermore, the need for deriving species-specific K_c -VI relationships is challenging when applying Landsat-scale data over heterogeneous landscapes and in areas that are very different from those where the empirical relationships were developed.

Besides knowing how much water crops need to thrive (a grower requirement), water resource managers need to know how much water was actually applied during a season (see [Section 4](#)). In many cases, VI methods will underestimate actual seasonal ET, neglecting precipitation events or irrigation water applied pre-emergence (where VI is near 0), and over-application in excess of requirements, where a significant fraction may be evaporated from the soil. [Fig. 4](#) shows ET maps developed over irrigated farmland determined using METRIC (TIR) and using NDVI alone. The major differences are in areas of low VI and high soil evaporation, which show uniform NDVI but a wide spread in LST due to surface soil moisture variations. Unlike TIR methods, VI methods give no information about ET after the crops/vegetation have senesced.

VI-only methods will tend to overestimate ET when stress develops rapidly, before biomass is able to adjust. This was verified by a study applying TSEB, METRIC and a reflectance-based crop coefficient model (cf. Eq. 3) over a rain-fed corn and soybean production region in Iowa during a prolonged dry-down period ([Gonzalez-Dugo et al., 2009](#)). TIR methods have the potential for providing early warning of impending drought-related crop failure/yield reductions, as signaled by elevated canopy temperatures, provided the TIR data can be collected at a reasonable temporal frequency.

3.4. LST as a soil moisture proxy indicator

In TIR-based ET models, moderate-resolution LST data serve as an effective proxy for field-scale soil moisture and antecedent precipitation/irrigation information, replacing the need for a priori soil water balance modeling required by dual crop coefficient models. At present, no other waveband or surface measurement network can provide soil moisture information at this critical spatial scale. [Hain et al. \(2009\)](#) demonstrated that available water fraction estimates related to the ratio of actual-to-potential ET (f_{PET}) derived from TIR remote sensing correlate well with observations from the Oklahoma Mesonet. Other groups have used relationships with TIR-derived evaporative fraction to map volumetric soil moisture ([Ahmad and Bastiaanssen, 2003; Bastiaanssen et al., 2000; Mohamed et al., 2004](#)). Triple collocation comparisons of TIR-based soil moisture estimates with microwave retrievals and soil moisture output from the Noah land-surface model conducted by [Hain et al. \(2011\)](#) demonstrate the value and skill added by the thermal band in diagnosing root-zone moisture conditions impacting transpiration rates, particularly in areas of dense vegetation cover. [Anderson et al. \(2011a\)](#) showed that anomaly patterns in f_{PET} over CONUS, mapped with ALEXI using GOES TIR data, agree well with rainfall anomalies – evidence that thermal remote sensing can provide surrogate moisture information even at continental scales.

In short, the TIR observation is an integrative, diagnostic indicator of the overall evaporative status of a patch of land-surface, requiring no *a priori* information of how or why that status evolved – much like a thermometer is used to diagnose the health status of the human body ([Anderson and Kustas, 2008](#)). Improved global monitoring of LST, as a fundamental earth science record covering a range in spatiotemporal scales, must be an integral component of future water resource satellite missions.

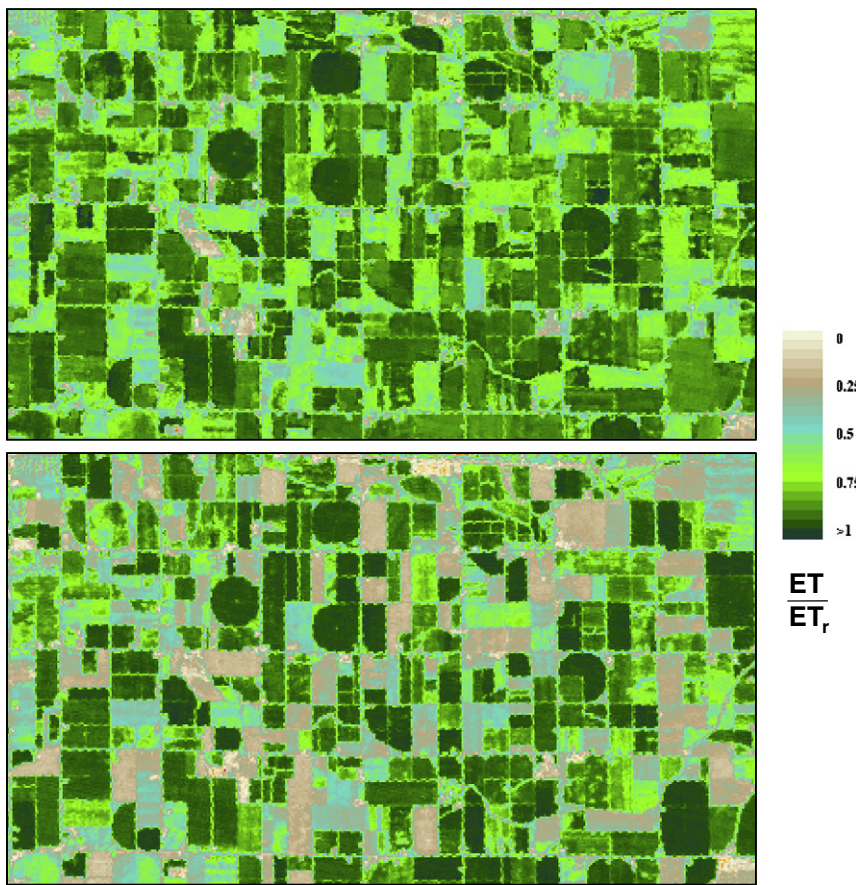


Fig. 4. Comparison of ET maps over an irrigated area in Idaho generated using the TIR-based METRIC approach (top), and using VI data only (bottom). The two approaches agree well for fields at very wet and dry conditions within the METRIC scene, but less well at intermediate moisture conditions. In these cases, the LST is too cold to be consistent with the low ET rates predicted by the VI method, presumably reflecting soil evaporation that is unaccounted for using VIs only.

4. Applications of moderate resolution ET

Based on demonstrated robustness and ability to monitor detailed structure over large areas, ET maps derived from moderate-resolution TIR imagery from the Landsat satellite series have been actively integrated into water resource management plans, particularly in the western US (Allen et al., 2005; Allen et al., 2007a; Bastiaanssen et al., 2005; Bastiaanssen et al., 2008). Moderate-resolution ET maps also have unique utility for monitoring ecosystem health, drought, and food security, and for evaluation of large scale hydrologic and climate models. Some of these applications are described below.

4.1. Water rights monitoring and compact negotiations

Such diverse observers of the 19th century American West as John Wesley Powell and Mark Twain warned that a lack of water would limit the settling of the West. Those observations are as true today as they were 150 years ago. Landsat-based ET information is beginning to move forward arguments over historical water use and potential versus actual ET by providing images of the spatial distribution of water consumption, often for individual fields to which water rights are tied. The nearly 30-year archive of TIR data from Landsat supports claims of use or nonuse of water and provides the means to develop and calibrate physical and economic models describing impacts of water consumption in agriculture.

The Idaho Department of Water Resources (IDWR) has already used Landsat TIR-based ET to make decisions regarding injury to senior water rights holders by junior pumpers (Kramber et al., 2010), and to identify individual users that are pumping groundwater at

rates in excess of their existing water rights (Fig. 5). Because water rights holdings are typically on the order of 800 by 800 m in dimension, Landsat-scale TIR is required to resolve water use associated with individual rights. IDWR and other western water management agencies are also investigating the potential for using long time-series of Landsat-based ET images to quantify multi-state depletions of river discharge as part of interstate stream compacts.

4.2. Ecosystem health and water requirements

Riparian, wetland, and other ground-water dependent plant communities are biologically important and fragile ecosystems that have widely varying vegetation type, density and water availability. These systems, in general, have uncertain water requirements and impacts on streamflow depletion. Furthermore, irrigation networks that have developed along waterways can adversely affect streamflow and fish populations. Moderate- to high-resolution satellite TIR data are essential to understanding the spatial distributions of ET in groundwater-dependent ecosystems, which often exist in narrow riparian corridors, and for assessing how concentrated evaporative losses from these systems impact basin-scale water budgets and native species.

4.2.1. Water consumption by salt cedar

Water consumption by riparian vegetation (cottonwoods) and irrigated fields along the Rio Grande south of Albuquerque, New Mexico is shown in Fig. 6, along with the relative spatial frequency distribution of annual ET by cottonwoods and invasive salt cedar for the same region, derived by sampling along a 50-km stretch of

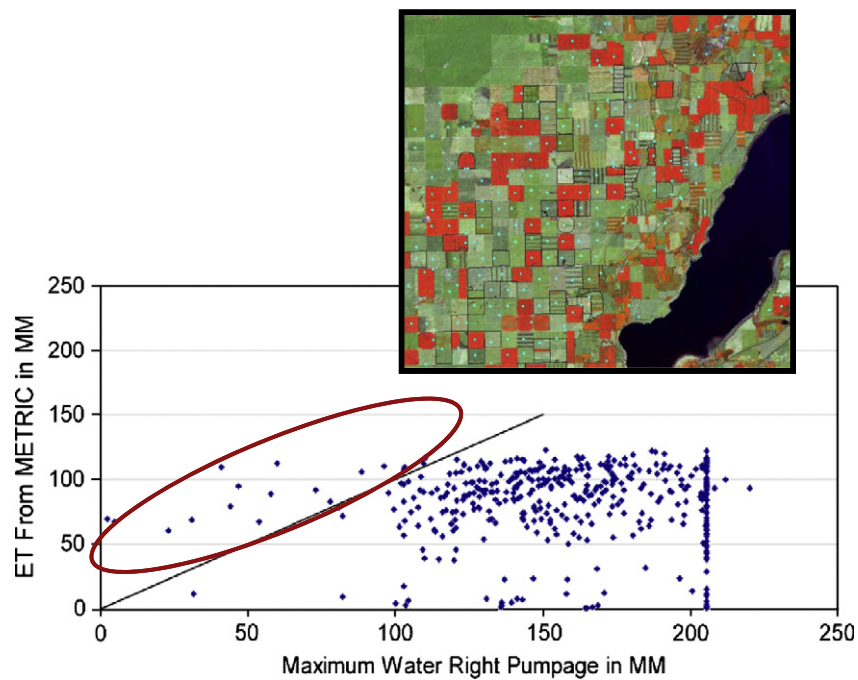


Fig. 5. Analysis of water rights compliance near the American Falls Reservoir of Idaho using METRIC ET. The scatter plot shows 17-day, cumulative water-use per water-right polygon versus the maximum possible pumpage allowed under terms of each water right. Points circled in red warrant further investigation because their ET exceeds the maximum righted level of pumpage. The line of points at 206 mm corresponds to the maximum duty of water for the 17-day duration of the analysis. The “duty of water” under the Prior Appropriation Doctrine is a measure of the amount of water needed to properly irrigate an area, corresponding to 0.02 cubic feet per second per acre in this case. Water-rights polygons are shown in the inset false-color image. Polygons are approximately 400 by 400 m in size. Blue dots represent locations of irrigation wells.v.

river. Salt cedar or Tamarisk was introduced to North America as a hardy ornamental, but lacking natural predators, the trees have spread throughout river corridors of the west, displacing more than 0.7 million ha of willows, cottonwoods and other native vegetation.

What is unknown is the amount of water that salt cedar consumes, estimated to range from 2 to 20 billion m³/year (Owens and Moore, 2007), thus having a 10-fold level of uncertainty. Based on early high estimates of consumptive use, widespread salt cedar removal

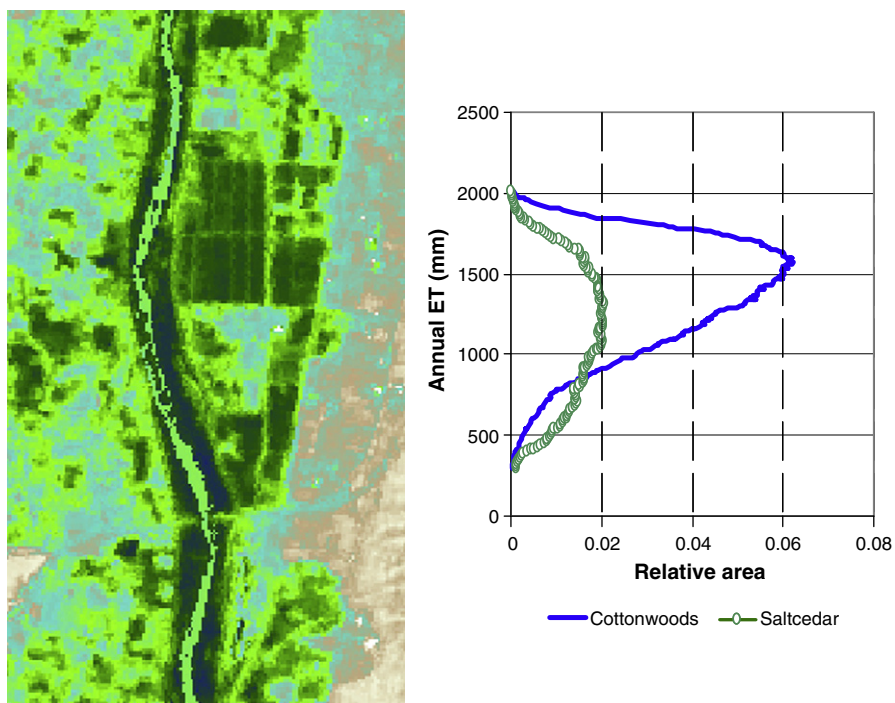


Fig. 6. Daily water consumption by riparian vegetation (cottonwoods) and from irrigated fields along the Rio Grande south of Albuquerque, New Mexico during 2002, mapped with METRIC using Landsat 7 (left). Darker green connotes higher ET. A relative frequency distribution of annual ET by cottonwoods and invasive salt cedar for the same region, derived by sampling along a 50-km stretch of river is shown on the right.

campaigns were instigated in the western US, along with release of a beetle that causes defoliation of salt cedar. However, these programs have not demonstrated significant conservation of water for human uses, and the beetle is now spreading to other river basins (Shafroth et al., 2010).

More research is needed on water consumption rates of salt cedar to develop a more effective management plan. Fig. 6 that shows water loss along the Rio Grande is highly spatially variable, depending on species, proximity to streambed, evaporation from soil caused by capillary rise from shallow water tables (discernable only with TIR), and vegetation health. Thermal remote sensing data from Landsat can be used to refine existing seasonal water-use estimates based on vegetation indices by better constraining the soil evaporation component of ET.

4.2.2. Water requirements for salmon habitat

The Snake and Salmon Rivers in Idaho (tributaries to the Columbia River) support populations of endangered anadromous fish – fish like salmon and steelhead that live in the ocean but migrate to freshwater for spawning. The watersheds feeding these rivers often do not supply enough water to meet the needs of both established irrigation and minimum stream flows for these endangered species. During drought years, irrigation often diverts the entire flow in a headwater stream.

Under a program funded by the Bonneville Power Administration and managed by the US Fish and Wildlife Service, the IDWR and National Marine Fisheries Service (NMFS) lease water rights from irrigators in the upstream Lemhi River basin to augment flows in the Salmon River and the larger Columbia River basin. To estimate potential for augmentation, planners needed to know the amount of ET from lands irrigated by specific water rights above certain points in the river. Before ET mapping information became available, the NMFS computed flow augmentation by simply adding up the total diversions from the Lemhi River. That number was unrealistically high because NMFS did not take into account the return of non-evaporated irrigation diversions back to the river. The IDWR used METRIC ET maps generated from Landsat TIR imagery, overlaid with water-right polygons, to convince NMFS that a realistic number for flow augmentation should be based on total consumptive use, not total diversion. Landsat thermal data contributed directly to a negotiated solution that protects endangered fish while at the same time protects the fair use of water by irrigators.

Similar work has been done in the Snake River basin where the IDWR and USBR have paid irrigators to leave water in the Snake

River to support minimum flow levels, using METRIC ET data to evaluate irrigators' claims for water diverted. In one instance, an irrigator used power consumption and pump performance curves for the year 2000 to calculate that 7570 acre-feet of water were diverted to irrigate 1690 acres, which is 4.48 acre-feet per acre or 1370 mm. However, the Department was willing to credit only the amount of water consumptively used, not the total diversion because the difference was return flow to the river. METRIC estimates based on Landsat TIR data supported a consumptive use estimate of only 980 mm during 2000. As a result, the irrigator chose not to participate in the buy-back program, and ET data directly supported decisions concerning the wise use of public money.

ET data have also been used to verify the effectiveness of water rights buy-backs. The Bell Rapids Irrigation Project near Hagerman, Idaho originally irrigated approximately 25,000 acres of cropland using high-lift pumps that lifted water 200 meters from the Snake River. The State of Idaho purchased the Project's water rights in 2005 for \$24.3 million. The USBR, in turn, leases the water from the State to increase flows for Snake River salmon recovery downstream, and the state uses the lease payments to recover the cost of the purchase. Fig. 7 shows Landsat-derived ET data for the irrigation seasons of 2000 and 2006, used to quantify the large change in ET before and after the water rights buyout.

4.2.3. Estimating impacts of groundwater extraction on phreatophytic communities

Many ecosystems with shallow groundwater tables are in hydrologic and hydraulic balance, with precipitation nearly equal to ET. These systems are generally fragile and can be damaged by decreases in water table caused by groundwater pumping. In Florida, groundwater pumping for municipal water supply has reduced the health of trees and shrubs that derive water supply during dry periods from groundwater. Thermally derived ET has been used to assess relative quantities of ET and tree health as well as to calibrate parameters in groundwater simulation models (Morse et al., 2005).

In Nevada, water sources for phreatophytic systems of sage brush, creosote brush and similar systems originate from adjacent mountain ranges. Water from snowmelt and infiltrated rain flows laterally underground toward valley centers where it feeds and sustains the deep-rooted vegetation systems. Large cities in Nevada are making plans to pump groundwater for municipal supplies, which may adversely affect the health of these ecosystems (Devitt et al., 2010).

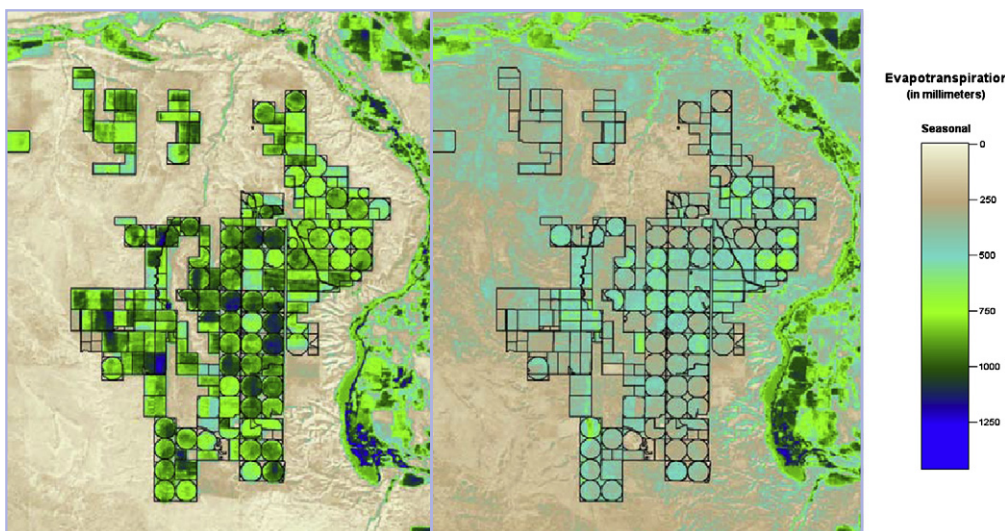


Fig. 7. ET from the 10,000 ha (25,000 acre) Bell Rapids irrigation project in southern Idaho in year 2000 (left) and 2006 (right) contrasting ET before and after a permanent buyout of irrigation rights by the State of Idaho in 2005. The 2006 image shows ET supplied by residual soil water stored during 2005.

Thermally based ET is necessary to map the spatially variable historical water consumption by the phreatophytes to set sustainable water yields and to monitor residual ET in the future.

4.3. Water use projections with changing land use

Idaho's Boise Valley grew in population from 257,000 in 1980 to 431,000 in 2000. Water planners need to understand how demands for water will be affected during the next 50 years by the transition of land from irrigated agriculture to residential, commercial, and industrial uses.

In 2000 and 2001, the USBR and IDWR cooperatively generated a land-use/land-cover (LULC) classification of the Boise River Valley for the year 2000 using 1:24,000-scale aerial photographs. The classification consists of twenty-four LULC classes in vector polygon format. In combination with Landsat-based METRIC ET data, the IDWR was able to estimate ET associated with specific LULC classes – valuable information that was not previously available (Morse et al., 2003). IDWR planners were able to use these data to understand how ET changes as land-use and land-cover change, providing a quantitative basis for making recommendations about water planning in the Boise Valley. Such analyses require moderate-resolution TIR data, collected at scales resolving nominal LULC class patches.

4.4. Drought monitoring

State and federal action agencies tasked with responding to drought in the US are increasingly requiring information at higher and higher spatial resolution. Currently, drought-related yield-loss compensation is distributed to individual growers based on very coarse-resolution assessments, such as recorded in the US Drought Monitor (USDM; www.drought.unl.edu/dm/monitor.html), while actual impacts on the ground can be much more localized. Tools for

monitoring drought impacts on a field-by-field basis will benefit both mitigation and compensation efforts.

Anderson et al. (2007a, 2011b) demonstrated that an Evaporative Stress Index (ESI) reflecting anomalies in the ratio of actual-to-potential ET (f_{PET}), generated with the ALEXI model at 10-km resolution using GOES imagery, reproduces spatial patterns in standard precipitation-based drought indices, while requiring no rainfall data (Fig. 8). Their results suggest that the LST inputs provide proxy information about soil moisture and rainfall conditions even in areas of dense vegetation cover. There are currently no techniques available for monitoring rainfall at sub-field scales over large areas, while microwave soil moisture retrievals operate at resolutions exceeding 10 km, and do not function well in areas of dense cover. Vegetation index is a slow response variable to moisture, showing decline only after the damage has been done. In contrast, moderate-resolution TIR imagery from Landsat has the potential to provide valuable early warning regarding soil moisture deficits and canopy stress at scales required for operational management, preceding detectable degradation in VIs.

The Landsat archive is the only source of moderate-resolution data that can be used to produce the long period of baseline ET data needed for drought monitoring. However, to be more effective, such applications will greatly benefit from an increase in the temporal frequency of TIR image acquisitions at moderate resolutions.

4.5. Food and water security

Seasonal ET and crop yields tend to be tightly correlated because carbon assimilation by plant canopies and transpiration fluxes are both regulated by stomatal conductance. Both yield and ET are reduced by pressures such as disease, insects, low fertility, soil and water salinity, and water shortage. These stressors cause stomatal closure, reducing evaporative cooling by transpiration, and increasing

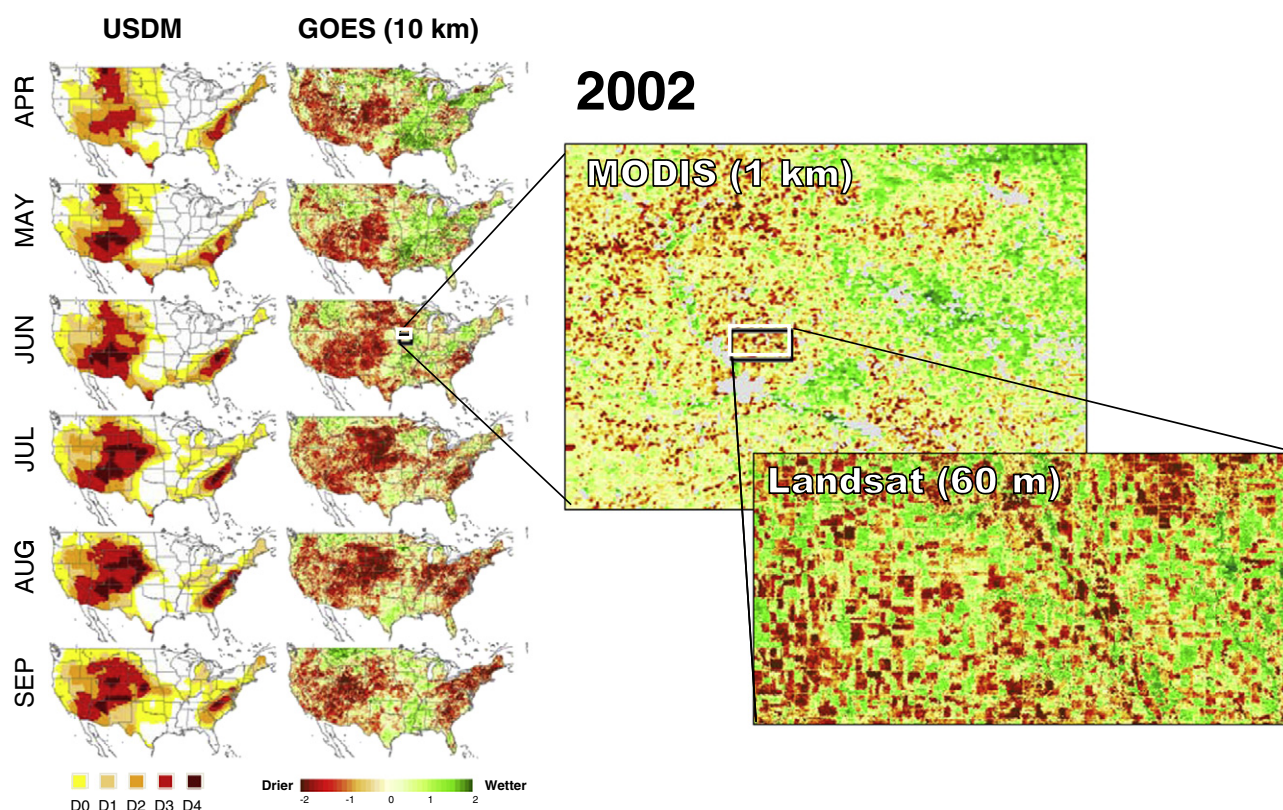


Fig. 8. Monthly drought conditions for April–September during 2002 recorded in the US Drought Monitor (USDM) and mapped with the thermal-based GOES ESI at 10-km resolution. Also shown are maps of f_{PET} generated with MODIS and Landsat TIR imagery, scaling down to moisture conditions in individual fields in central Iowa.

canopy temperature, which can be observed from a satellite sensor in the thermal waveband. Satellite TIR images and derived ET maps have the potential for providing early warning of impending crop failure and food shortages, even before there is a noticeable decline in green vegetation cover fraction and associated shortwave vegetation indices (VI). Furthermore, the ratio of yield to water consumption is an effective indicator of crop water use efficiency (Howell, 2001). Therefore, frequent TIR monitoring at moderate spatial resolution should be an essential component of a global food security satellite system.

A dedicated earth observation (EO) system for water and food security will be imperative as we try to improve the global efficiency of conversion of water into food, which will be needed to produce the 70% increase in food needs projected over the next 40 years. Such an EO system will facilitate monitoring of agricultural vegetation health, distribution, and biomass production in association with water consumption. The system will also promote more sustainable management of land- and water resources. Many areas of the globe have reached or exceeded sustainable levels of water exploitation, with groundwater levels in decline and with streamflows well below the needs of ecosystems. The spatial diversity of precipitation, vegetation and water use mandates global-scale mapping of water consumption at both national levels and at local project implementation levels, with high spatial and temporal resolution.

Neither individuals nor organizations can manage what they cannot measure. Countries cannot know how much irrigation water is effectively used to produce food unless they can detect ET from crop vegetation systems from space. Significant improvements in our ability to monitor and develop knowledge of consumptive water use and global food production can only be achieved using multi-spectral and thermal observations.

4.6. Evaluation of regional and global models

Evapotranspiration is an integrative indicator of climate change, being sensitive to changes in precipitation and temperature, and radiation load. ET is the key link between the global energy and water cycles, and has a strong influence on regional weather and precipitation recycling. Accurate records of consumptive water use patterns around the globe will be critical to the development of adaptation strategies, allowing us to identify areas where water availability will be most threatened. However, the global climate models (GCMs) used to develop these future scenarios have not been well validated for ET and they are notoriously error prone, being very sensitive to errors in

the prescribed precipitation, soil texture and vegetation water use characteristics (e.g., Mueller et al., 2011; Seneviratne et al., 2010). Moderate-resolution remotely sensed ET fields will be critical for GCM validation, as they provide the only viable bridge between the tower flux footprint scale, often on the order of 100 m, and the GCM grid scale of 100 s of km (Fig. 9). Fig. 3 exemplifies the importance of validating at the observation scale.

Unlike prognostic climate models, remote sensing ET models cannot be run into the future because they are founded on a diagnostic measure of the current land-surface temperature. Still, diagnostic models such as SEBAL, METRIC and ALEXI/DisALEXI can be used to validate and calibrate surface conductance and rooting depth formulations and soil evaporation components used in many climate models, and in regional land-surface models (LSMs). ALEXI/DisALEXI are being used as an independent assessment of prognostic hydrologic evaluations generated with the Noah LSM (Ek et al., 2003) over the Nile River Basin in support of basin-scale water management tools (Anderson et al., 2011c). In prognostic LSMs, non-precipitation-related moisture inputs to the land-surface evaporation, such as from irrigation or near-surface water tables, must be known a priori and explicitly represented in the model. The TIR-based remote sensing ET maps inherently capture these contributions to the evaporative flux without prior knowledge, and facilitate estimation of diversions along the river that support irrigated agriculture (e.g. in the Nile Delta), and additional evaporative losses from extensive wetland areas like the Sudd in southern Sudan. Landsat disaggregation of ALEXI 6-km fluxes, generated with LST products from the Meteosat geostationary satellite, will give detailed information about the complex water distribution systems that have developed along the Nile (Fig. 10).

GCM and LSM performance must be rigorously evaluated under current conditions before future scenario projections of water and energy exchange can be considered reliable. The global coverage and long-term archive of TIR imagery provided by the Landsat satellite series is a valuable asset to climate change research.

5. Improving the spatiotemporal resolution of ET information

5.1. Thermal sharpening

Over many landscapes, TIR image resolution (nominally 60–120 m for Landsat) can be improved by fusing information from the short-wave bands, instrumented at 30-m resolution on Landsat. Thermal sharpening algorithms (Agam et al., 2008; Anderson et al., 2004; Kustas et al., 2003; Merlin et al., 2010; Trezza et al., 2008) exploit

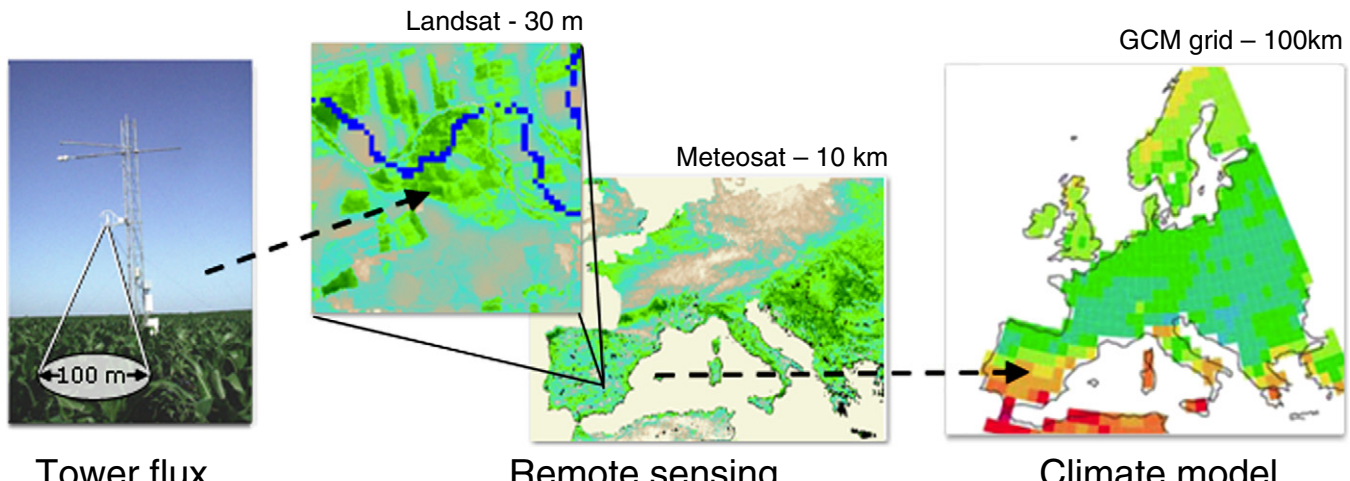


Fig. 9. Schematic showing process for upscaling from the flux tower footprint scale (~100 m) to the GCM grid scale (100 km), using TIR remote sensing from Landsat and Meteosat as intermediate steps.

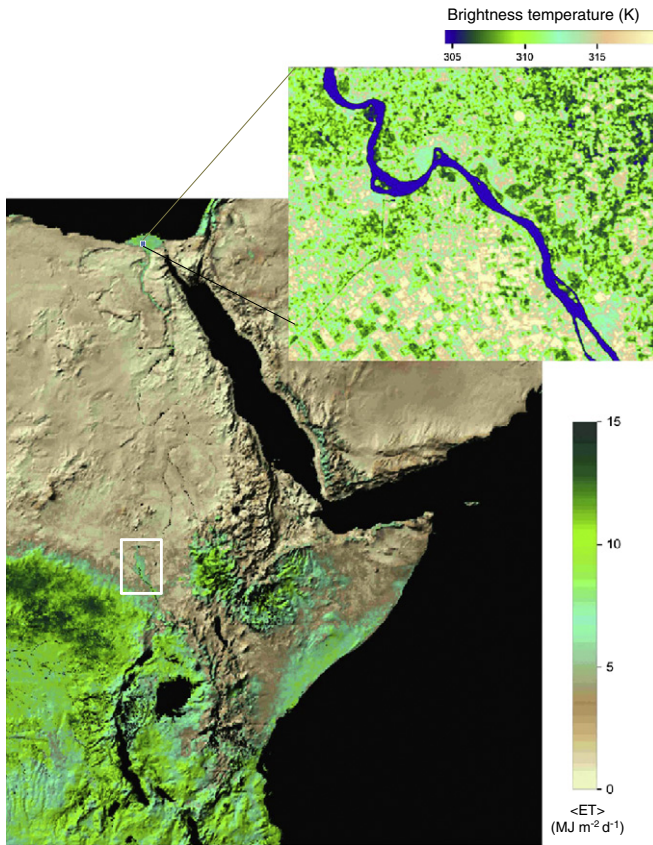


Fig. 10. Monthly averaged daily ET over the Nile River Basin, generated with ALEXI using Meteosat LST products for May 2009, along with a brightness temperature map from Landsat 5 showing the complex irrigation system in the Nile Delta. Evaporation from the Sudd wetland in southern Sudan is also detected by the TIR modeling scheme (white box).

the strong relationship that typically exists between land-surface temperature and vegetation indices (VIs) derived from vis/NIR data (Agam et al., 2008; Anderson et al., 2004; Kustas et al., 2003; Merlin et al., 2010; Trezza et al., 2008). Under moisture-limiting conditions, denser vegetation cover tends to be associated with lower surface temperatures due to cooling by transpiration. On the other hand, when vegetation growth is energy-limited (insolation or ambient temperature), VI and LST are often positively correlated (Karnieli et al., 2010). Sharpening algorithms generally determine a locally representative LST-VI relationship at the coarser native resolution of the TIR imagery, then apply that relationship to the VI image to distribute LST at the finer scale of the shortwave bands, taking care to conserve the original thermal radiation flux emission. Merlin et al. (2010) and Inamdar and French (2009) further enhanced the standard sharpening algorithm to account for impacts of non-green vegetation (e.g. stubble or residue) on surface temperature variations.

Anderson et al. (2004) investigated the impact of thermal sharpening on latent heat flux maps over agricultural landscapes in Oklahoma, derived from Landsat TIR imagery sharpened to 30-m resolution. The sharpening procedure successfully enhanced fine spatial details such as field borders, residential streets, and golf-course fairways (Fig. 11). Sharpened ET retrievals stemming from sharpened TIR improves estimation of field-wide ET associated with water rights. The improvement in ET estimates over an irrigated landscape is demonstrated in Fig. 12, where definition in Landsat-derived ET along the edges of center pivot fields has been sharpened to 30-m resolution.

Sharpening works well in landscapes where moisture variations are well-resolved at the native TIR resolution, and sub-pixel TIR variability is correlated with vegetation cover in a locally consistent way.

This constraint will start to break down for coarser resolution TIR data sources such as MODIS (1 km) over landscapes with sub-kilometer scale moisture variations, such as in irrigated agricultural areas (Agam et al., 2008). In addition, field-to-field variability in soil moisture in irrigated areas, especially under conditions of low vegetation cover, complicates the sharpening process and can increase uncertainty (Trezza et al., 2008).

These results suggest that while thermal sharpening is a valuable tool for enhancing spatial information content in TIR imagery, it does not replace the need for TIR data collection at the sub-field scale as currently provided by Landsat. At the 100-m scale of Landsat, most moisture variations are resolved and the potential for sharpening to 30 m over many landscapes is high. Still, in areas where both positive and negative TIR-VI correlations exist within one landscape (e.g., in the Alaskan tundra), or for some other reason TIR-VI is not well correlated, more sophisticated sharpening algorithms will be needed that accommodate spatially varying relationships between temperature and vegetation cover (Jeganathan et al., 2011). Ideally, future satellite systems will be developed providing TIR at a native resolution of 30 m or finer.

5.2. Synergistic use of moderate and coarse resolution TIR imagery

While MODIS-like data cannot supplant the need for Landsat-scale TIR imagery for many applications, they can be effectively used to constrain temporal interpolation of moderate resolution ET fields. The standard technique currently used to generate daily, monthly and seasonal ET estimates at the field scale is to directly interpolate between infrequent Landsat-derived ET images, conserving some quantity such as the ratio of actual ET to a weather-based reference ET during the intervening gap to capture evaporative response to temporal variability in radiation load and atmospheric demand (e.g., Allen et al., 2007b). In perpetually cloudy regions, however, one may obtain only two or three clear Landsat TIR images per growing season, providing insufficient temporal sampling to reliably assess daily and cumulative water consumption.

Using new data fusion techniques, such as the Spatial Temporal Adaptive Reflectance Fusion Model (STARFM) developed by Gao et al. (2006), we can improve seasonal moderate-resolution ET estimates by integrating daily ET information at lower resolution from wide-swath sensors like MODIS with periodic moderate-resolution ET maps from Landsat. The STARFM approach was originally developed to blend surface reflectance between high spatial resolution Landsat and high temporal resolution MODIS data, but works well with multi-scale ET imagery as well. The approach uses spectrally similar pixels in Landsat images and temporal changes determined from MODIS. STARFM predicts Landsat-resolution ET at MODIS acquisition dates based on a deterministic weighting function of spectral similarity, temporal difference, and spatial distance, determined from available Landsat-MODIS image pairs.

Fig. 13 shows an example of ET data fusion using ALEXI/DisALEXI. In the fused images between Landsat acquisitions on days 328 and 336, diurnal information about the daily available energy curve is provided by GOES, daily variability in ET at the kilometer scale by MODIS, while field-scale patterns provided by 8-day sampling from the combined Landsat 5 and 7 satellites. The MODIS ET maps capture coarser scale variability in moisture conditions between Landsat overpasses, due to precipitation events or evolving drought conditions. Further studies are underway to quantify prediction accuracy over seasonal timescales.

6. Optimal satellite configuration for water resource management

The Landsat satellite system has been the operational EO system of choice for ET determination at moderate resolution. Since 1982, the Landsat system has recorded continuous coverage, especially over North America, of thermal imagery at 60–120 m resolution and at

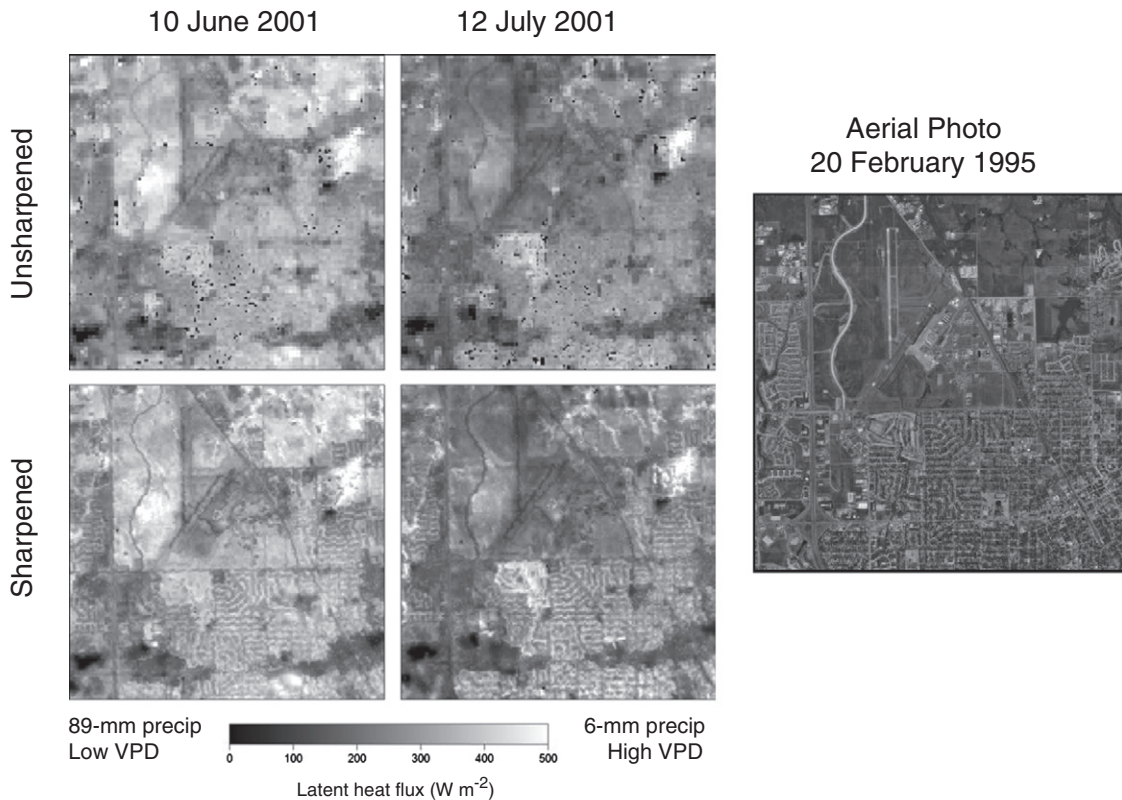


Fig. 11. Impact of thermal sharpening on latent heat flux maps generated with Landsat 7 TIR data over the city of Norman, OK on 10 June and 12 July 2001. In the 2 weeks prior to June 10, 89 mm of rain was recorded at the Norman weather station, and ET was high across the area. In the following month, however, precipitation dropped off dramatically. On July 12, high ET was maintained only in riparian areas and areas that were receiving regular irrigation (e.g., residential lawns, the golf course just SW of center). In these areas, ET was higher in July than in June due to higher vapor pressure deficits (VPD). This type of detailed analysis is greatly facilitated by the sharpening process.

30 m in the visible and near infrared (vis/NIR) bands. Of the two remaining Landsat satellites, Landsat 5 is nearly worn out, and Landsat 7 is damaged. Landsat 8 is scheduled for launch in December 2012 and will soon be the only active Landsat, with a 16-day revisit interval. Multiple concurrently operating Landsat systems equipped with thermal imagers are needed to accurately track water consumption by ET, which changes rapidly with vegetation development, water supply and precipitation events at a relatively fine scale.

Allen (2010, personal communication) demonstrated the importance of multiple, concurrent Landsat satellites to mitigate the effects of clouds on monthly and seasonal ET computations. The analysis used 26 years of Landsat 5 and 10 years of Landsat 7 images for two Landsat paths in southern Idaho, a relatively cloud-free region. The target requirement specified for monthly ET production was a minimum of one cloud-free image for any specific area of interest at least once each 32 days during the growing season. Allen showed that a single satellite having a 16-day return time achieved this requirement for only one year (4%) to two years (8%) out of the 26-year archive. With a second satellite having the same 16-day return time, but with an 8-day offset from the first satellite, the number of years successfully meeting this requirement increased to four years out of ten (40%) for both paths. With a 4-day return, the requirement of one monthly clear-sky image was met in 70 to 80% of years. More humid regions of the US, such as the Midwest, have more cloudy images and will require an even shorter image time interval for high levels of success.

It is clear that Landsat 8 needs to be joined by additional Landsat systems or other quality EO satellites equipped with moderate-resolution thermal imagers. A virtual satellite constellation needs to be assembled, comprised of multi-spectral systems including thermal and vis/NIR instruments. While some such systems have been launched (e.g., the

China-Brazil Earth Resources Satellite – CBERS, and the Chinese HJ-1B satellite), absence of a free and open access data policy impedes the use of these datasets, and in some cases the data quality is poorer than required. No other systems with high quality thermal imagers at moderate resolution (<120 m) are on the horizon except for the proposed Hyperspectral Infrared Imager (HyspIRI; NASA-JPL, 2008) research satellite mission (global land-surface coverage at 60-m resolution and 5-day revisit in multiple TIR bands). The foreseeable consequences are that EO-assisted water monitoring and management will not happen at the global scale for some time. In addition, water management entities, especially those that are completely government supported, are typically reluctant to invest in developing and adopting new technologies that are based on ‘research’ satellites and programs, that tend to have relatively short life spans and patchy coverage (e.g., ASTER), as opposed to ‘operational’ programs such as Landsat that have more assurance for future operation.

In future Landsat missions, a minimum four-day return time is recommended for successful ET retrievals over large portions of the globe. The four-day return time can be accomplished using four time-staggered satellites having the current 160-km path width design. The same return time can be accomplished with two satellites having double that path width. This would require expanding the view angle to a maximum of about 15° from nadir, which may be a maximum tolerable view angle to minimize negative effects of pixel information distortion such as those that plague the larger view angles of MODIS (Fig. 1). Furthermore, coordination between the orbits of Landsat and satellites carrying the MODIS follow-on instrument (VIIRS) would facilitate ET data fusion (Section 5.2), significantly enhancing the information content provided by either instrument operating in isolation.

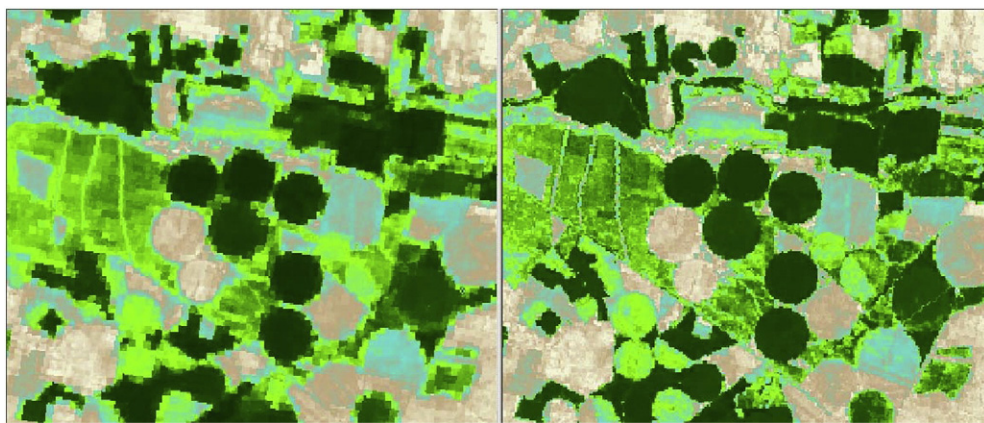


Fig. 12. Evapotranspiration from irrigated fields in central Spain during 2005 derived from a Landsat 5 image using the METRIC model prior to sharpening (left) and following sharpening (right) of TIR from 120 m to 30 m.

7. Conclusions

Significant progress has been made over the past two decades in moving TIR-based ET monitoring to a position where it is operationally and economically feasible, providing large-area ET information at accuracies and spatiotemporal resolutions required for many practical water resource applications. The moderate-resolution TIR image archive collected with the Landsat satellite series since 1982 provide an unequalled global view of changing water availability and consumption patterns at scales where humans are actively modifying the natural water cycle. Such information will be critical as we plan strategies for adapting to future changes in freshwater resources.

Moving forward, the power of Landsat TIR image acquisition for monitoring water use will be significantly improved by simultaneous flight of multiple Landsat satellites, and by doubling the current swath width of data collection. TIR imaging should be collocated with vis/NIR

imaging sensors, so that the vegetation cover and albedo information used in ET models is well registered with the TIR imagery in both time and space and can be easily ingested by management agencies. Furthermore, we recommend careful coordination of future Landsat missions with coarser resolution operational TIR acquisitions, such as from the MODIS follow-on VIIRS to fly on board the NPOESS Preparatory Project (NPP) satellite and the Joint Polar Satellite System (JPSS) satellites. A late-morning overpass by VIIRS, similar to the Landsat overpass time, would facilitate synergistic use of these instruments and greatly improve the spatiotemporal resolution of derived ET products.

For action agencies to be willing to invest the time and resources required to actively integrate remote sensing products into their management strategies, there must be an assurance that the satellite imaging capabilities will be maintained well into the future. Therefore, it is critical that planning for next generation Landsat systems begin now, and that the Landsat program be effectively transferred

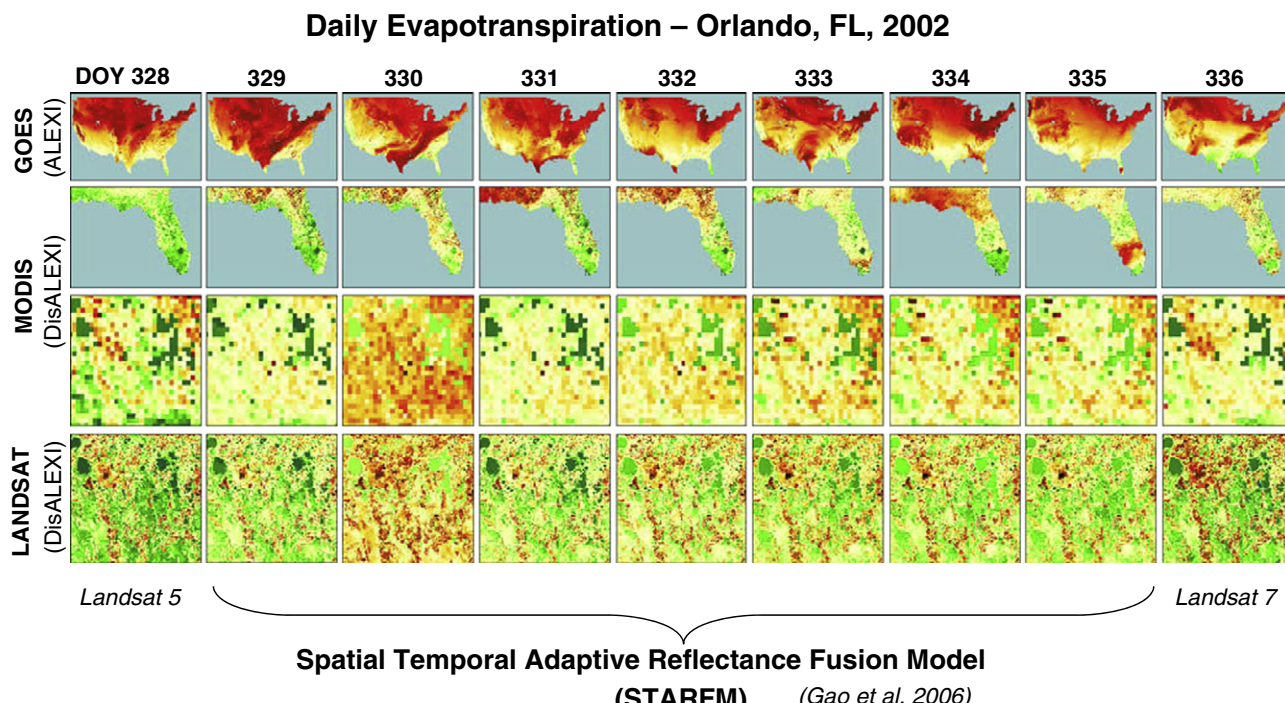


Fig. 13. Example of Landsat/MODIS/GOES ET data fusion, showing maps of daily ET from ALEXI at 10-km resolution (top row), from DisALEXI using MODIS TIR at 1-km resolution (middle rows), and from the STARFM data fusion algorithm, fusing information from DisALEXI using Landsat TIR sharpened to 30-m resolution (bottom row). Red indicates low ET, while green indicates high values. Landsat-scale maps for day of year (DOY) 329–335 were generated with STARFM. From [Anderson et al. \(2011b\)](#).

from NASA – a research agency – and integrated into an operational agency such as USGS.

Acknowledgements

Development of METRIC algorithms and applications has been supported by the Idaho Agricultural Experiment Station, the Idaho Dept. Water Resources, NASA, USGS, USDA, NSF EPSCoR and Raytheon Company, with substantial guidance by Dr. Wim Bastiaanssen of WaterWatch, Wageningen, the Netherlands and feedback by Mr. William Kramber, IDWR. Development of ALEXI/DisALEXI has been supported by NASA, NOAA, and USDA. We acknowledge the support of the Western States Water Council in sustaining US capacity in moderate resolution TIR. USDA is an equal opportunity provider and employer.

References

- Agam, N., Kustas, W. P., Anderson, M. C., Li, F., & Colaizzi, P. D. (2008). Utility of thermal image sharpening for monitoring field-scale evapotranspiration over rainfed and irrigated agricultural regions. *Journal of Geophysical Research, Letters*, 35, doi: 10.1029/2007GL032195.
- Ahmad, M., & Bastiaanssen, W. G. M. (2003). Retrieving soil moisture storage in the unsaturated zone using satellite imagery and bi-annual phreatic surface fluctuations. *Irrigation and Drainage Systems*, 17, 141–161.
- Allen, R. G., Pereira, L. S., Raes, D., & Smith, M. (1998). Crop evapotranspiration: Guidelines for computing crop water requirements. *United Nations FAO, irrigation and drainage paper 56, 300 pp, Rome, Italy*.
- Allen, R. G., Tasumi, M., Morse, A. T., & Trezza, R. (2005). A Landsat-based energy balance and evapotranspiration model in western U.S. water rights regulation and planning. *Journal of Irrigation and Drainage Systems*, 19, 251–268.
- Allen, R. G., Tasumi, M., Morse, A., Trezza, R., Wright, J. L., Bastiaanssen, W. G. M., et al. (2007a). Satellite-based energy balance for mapping evapotranspiration with internalized calibration (METRIC) – Applications. *ASCE Journal of Irrigation and Drainage Engineering*, 133, 395–406.
- Allen, R. G., Tasumi, M., & Trezza, R. (2007b). Satellite-based energy balance for mapping evapotranspiration with internalized calibration (METRIC) – Model. *Journal of Irrigation and Drainage Engineering*, 133(4), 380 10.1061/(ASCE)0733-9437.
- Anderson, M. C., Hain, C. R., Wardlow, B., Mecikalski, J. R., & Kustas, W. P. (2011a). Evaluation of a drought index based on thermal remote sensing of evapotranspiration over the continental U.S. *Journal of Climate*, 24, 2025–2044.
- Anderson, M. C., & Kustas, W. P. (2008). Thermal remote sensing of drought and evapotranspiration. *Eos Transactions, American Geophysical Union*, 89, 233–234.
- Anderson, M. C., Kustas, W. P., & Norman, J. M. (2007a). Upscaling flux observations from local to continental scales using thermal remote sensing. *Agronomy Journal*, 99, 240–254.
- Anderson, M. C., Norman, J. M., Diak, G. R., Kustas, W. P., & Mecikalski, J. R. (1997). A two-source time-integrated model for estimating surface fluxes using thermal infrared remote sensing. *Remote Sensing of Environment*, 60, 195–216.
- Anderson, M. C., Norman, J. M., Kustas, W. P., Houborg, R., Starks, P. J., & Agam, N. (2008). A thermal-based remote sensing technique for routine mapping of land-surface carbon, water and energy fluxes from field to regional scales. *Remote Sensing of Environment*, 112, 4227–4241.
- Anderson, M. C., Norman, J. M., Kustas, W. P., Li, F., Prueger, J. H., & Mecikalski, J. M. (2005). Effects of vegetation clumping on two-source model estimates of surface energy fluxes from an agricultural landscape during SMACEX. *Journal of Hydrometeorology*, 6, 892–909.
- Anderson, M. C., Norman, J. M., Mecikalski, J. R., Otkin, J. P., & Kustas, W. P. (2007b). A climatological study of evapotranspiration and moisture stress across the continental U.S. based on thermal remote sensing: I. Model formulation. *Journal of Geophysical Research*, 112, D10117 10110.11029/12006JD007506.
- Anderson, M. C., Norman, J. M., Mecikalski, J. R., Otkin, J. P., & Kustas, W. P. (2007c). A climatological study of evapotranspiration and moisture stress across the continental U.S. based on thermal remote sensing: II. Surface moisture climatology. *Journal of Geophysical Research*, 112, D11112 11110.11029/12006JD007507.
- Anderson, M. C., Norman, J. M., Mecikalski, J. R., Torn, R. D., Kustas, W. P., & Basara, J. B. (2004). A multi-scale remote sensing model for disaggregating regional fluxes to micrometeorological scales. *Journal of Hydrometeorology*, 5, 343–363.
- Anderson, M. C., et al. (2011b). Mapping daily evapotranspiration at field to continental scales using geostationary and polar orbiting satellite imagery. *Hydrology and Earth System Science*, 15, 223–239.
- Bastiaanssen, W. G. M., Menenti, M., Feddes, R. A., & Holtslag, A. A. M. (1998). A remote sensing surface energy balance algorithm for land (SEBAL); 1. formulation. *Journal of Hydrology*, 212–213, 198–212.
- Bastiaanssen, W. G. M., Molden, D. J., & Makin, I. W. (2000). Remote sensing for irrigated agriculture: Examples from research and possible applications. *Agricultural Water Management*, 46, 137–155.
- Bastiaanssen, W. G. M., Noordman, E. J. M., Pelgrum, H., Davids, G., Thoreson, B. P., & Allen, R. G. (2005). SEBALmodel with remotely sensed data to improve water resources management under actual field conditions. *ASCE Journal of Irrigation and Drainage Engineering*, 131, 85–93.
- Bastiaanssen, W. G. M., Pelgrum, H., Soppe, R. W. O., Allen, R. G., Thoreson, B. P., & Teixeira, A. H. d. C. (2008). Thermal-infrared technology for local and regional irrigation analyses in horticultural systems. *Acta Horticulturae*, 792, 33–46.
- Bausch, W. C. (1995). Remote sensing of crop coefficients for improving the irrigation scheduling of corn. *Agricultural Water Management*, 27, 55–68.
- Bausch, W. C., & Neale, C. M. U. (1987). Crop coefficients derived from reflected canopy radiation: A concept. *Transactions of ASAE*, 30, 703–709.
- Bausch, W. C., & Neale, C. M. U. (1989). Spectral inputs improve corn crop coefficients and irrigation scheduling. *Transactions of ASAE*, 32, 1901–1908.
- Blonquist, J. M., Norman, J. M., & Bugbee, B. (2009). Automated measurement of canopy stomatal conductance based on infrared temperature. *Agricultural and Forest Meteorology*, 149, 2183–2197.
- Cammalleri, C. M. C. Anderson, G. Ciraolo, G. D'Urso, W. P. Kustas, G. La Loggia, and M. Minacapilli (in review). Practical applications of the remote sensing-based two-source algorithm for surface energy fluxes mapping without in-situ air temperature observations, *Remote Sens. Environ.*
- Carlson, T. N. (1986). Regional-scale estimates of surface moisture availability and thermal inertia using thermal measurements. *Remote Sensing Review*, 1, 197–247.
- Carlson, T. N. (2007). An overview of the “triangle method” for estimating surface evapotranspiration and soil moisture from satellite imagery. *Sensors*, 7, 1612–1629.
- Cleugh, H. A., Leuning, R., Mu, G., & Running, S. W. (2007). Regional evaporation estimates from flux tower and MODIS satellite data. *Remote Sensing of Environment*, 106, 285–304.
- Devitt, D. a., Fenstermaker, L. F., Young, M. H., Conrad, B., Baghzouz, M., & Bird, B. M. (2010). Evapotranspiration of mixed shrub communities in phreatophytic zones of the Great Basin region of Nevada (USA). *Ecohydrology Wiley online*.
- Diak, G. R., & Stewart, T. R. (1989). Assessment of surface turbulent fluxes using geostationary satellite surface skin temperatures and a mixed layer planetary boundary layer scheme. *Journal of Geophysical Research*, 94, 6357–6373.
- Ek, M. B., Mitchell, K. E., Lin, Y., Rogers, E., Grunmann, P., Koren, V., et al. (2003). Implementation of Noah land surface model advances in the National Centers for Environmental Prediction operational mesoscale Eta model. *Journal of Geophysical Research*, 108(D22), 8851, doi:10.1029/2002JD003296.
- Gao, F., Masek, J., Schwaller, M., & Hall, F. G. (2006). On the blending of the Landsat and MODIS surface reflectance: predicting daily Landsat surface reflectance. *IEE Trans. Geosci. Remote. Sens.*, 44, 2207–2218.
- Gonzalez-Dugo, M. P., Neale, C. M. U., Mateos, L., Kustas, W. P., Prueger, J. H., Anderson, M. C., et al. (2009). A comparison of operational remote sensing-based models for estimating crop evapotranspiration. *Agricultural and Forest Meteorology*, 149, 1843–1853.
- Hain, C. R., Mecikalski, J. R., & Anderson, M. C. (2009). Retrieval of an available water-based soil moisture proxy from thermal infrared remote sensing. Part I: Methodology and validation. *Journal of Hydrometeorology*, 10, 665–683.
- Hain, C. R., Crow, W. T., Mecikalski, J. R., Anderson, M. C., & Holmes, T. (2011). An inter-comparison of available soil moisture estimates from thermal infrared and passive microwave remote sensing and land surface modeling. *Journal of Geophysical Research*, 116, D15107, doi:10.1029/2011JD015633.
- Hall, F. G., Huemmrich, K. F., Goetz, S. J., Sellers, P. J., & Nickerson, J. E. (1992). Satellite remote sensing of surface energy balance: Success, failures and unresolved issues in FIFE. *Journal of Geophysical Research*, 19 061–019,089.
- Howell, T. A. (2001). Enhancing water use efficiency in irrigated agriculture. *Agronomy Journal*, 93, 281–289.
- Hunsaker, D. J., Pinter, P. J., Barnes, E. M., & Kimball, B. A. (2003). Estimating cotton evapotranspiration crop coefficients with a multispectral vegetation index. *Irrigation Science*, 22, 95–104.
- Hunsaker, D. J. (1999). Basal crop coefficients for water use for early maturity cotton. *Transactions of ASAE*, 42, 927–936.
- Hunsaker, D. J., Pinter, P. J., & Cai, H. (2003). Alfalfa basal crop coefficients for FAO-56 procedures in the desert southwestern US. *Transactions of ASAE*, 45, 1799–1815.
- Inamdar, A. K., & French, A. N. (2009). Disaggregation of GOES land surface temperatures using surface emissivity. *Geophysical Research Letters*, 36, L02408 02410.1029/2008GL036544.
- Irons, J. R., Dwyer, J. L., & Barsi, J. A. (2012). The next Landsat satellite: The Landsat Data Continuity Mission. *Remote Sensing of Environment*, 122, 11–21 (this issue).
- Jeganathan, C., Hamm, N. A. S., Mukherjee, S., Atkinson, P. M., Raju, P. L. N., & Dadhwali, V. K. (2011). Evaluating a thermal image sharpening model over a mixed agricultural landscape in India. *International Journal of Applied Earth Observation and Geoinformation*, 13, 178–191.
- Jones, H. G., & Leinonen, I. (2003). Thermal imaging for the study of plant water relations. *Journal of Agricultural Meteorology*, 59, 205–217.
- Jones, H. G., Stoll, M., Santos, T., de Sousa, C., Chaves, M. M., & Grant, O. M. (2002). Use of infrared thermography for monitoring stomatal closure in the field: Application to grapevine. *Journal of Experimental Botany*, 53, 2249–2260.
- Kalma, J. D., McVicar, T. R., & McCabe, M. F. (2008). Estimating land surface evaporation: A review of methods using remotely sensed surface temperature data. *Survey Geophysical* 10.1007/s10712-10008-19037-z.
- Karnieli, A., Agam, N., Pinker, R. T., Anderson, M. C., Imhoff, M. L., Gutman, G. G., et al. (2010). Use of NDVI and land surface temperature for drought assessment: Merits and limitations. *Journal of Climate*, 23, 618–633.
- Kramber, W. J., Morse, A., & Allen, R. G. (2010). Mapping evapotranspiration: A remote sensing innovation. *Photogrammetric Engineering and Remote Sensing*, 76, 6–10.
- Kustas, W. P., Anderson, M. C., French, A. N., & Vickers, D. (2006). Using a remote sensing field experiment to investigate flux footprint relations and flux sampling distributions for tower and aircraft-based observations. *Advances in Water Resources*, 29, 355–368.

- Kustas, W. P., Diak, G. R., & Norman, J. M. (2001). Time difference methods for monitoring regional scale heat fluxes with remote sensing. *Land Surface Hydrology, Meteorology, and Climate: Observations and Modeling*, 3, 15–29.
- Kustas, W. P., Humes, K. S., Norman, J. M., & Moran, M. S. (1995). Single-and dual-source modeling of surface energy fluxes with radiometric surface temperature. *Journal of Applied Meteorology*, 35, 110–121.
- Kustas, W. P., & Norman, J. M. (1999). Evaluation of soil and vegetation heat flux predictions using a simple two-source model with radiometric temperatures for partial canopy cover. *Agricultural and Forest Meteorology*, 94, 13–29.
- Kustas, W. P., & Norman, J. M. (2000). A two-source energy balance approach using directional radiometric temperature observations for sparse canopy covered surfaces. *Agronomy Journal*, 92, 847–854.
- Kustas, W. P., Norman, J. M., Anderson, M. C., & French, A. N. (2003). Estimating subpixel surface temperatures and energy fluxes from the vegetation index-radiometric temperature relationship. *Remote Sensing of Environment*, 85, 429–440.
- Leinonen, I., Grant, O. M., Tagliafavia, C. P. P., Chaves, M. M., & Jones, H. G. (2006). Estimating stomatal conductance with thermal imagery. *Plant, Cell & Environment*, 29, 1508–1518.
- Li, F., Kustas, W. P., Anderson, M. C., Prueger, J. H., & Scott, R. L. (2008). Effect of remote sensing spatial resolution on interpreting tower-based flux observations. *Remote Sensing of Environment*, 112, 337–349.
- Li, F., Kustas, W. P., Prueger, J. H., Neale, C. M. U., & Jackson, T. J. (2005). Utility of remote sensing based two-source energy balance model under low and high vegetation cover conditions. *Journal of Hydrometeorology*, 6, 878–891.
- McNaughton, K. G., & Spriggs, T. W. (1986). A mixed-layer model for regional evaporation. *Boundary-Layer Meteorology*, 44, 262–288.
- Merlin, O., Duchemin, B., Hagolle, O., Jacob, F., Coudert, B., Chehbouni, A., et al. (2010). Disaggregation of MODIS surface temperature over an agricultural area using a time series of Formosat-2 images. *Remote Sensing of Environment*, 114, 2500–2512.
- Mohamed, Y. A., Bastiaanssen, W. G. M., & Savenije, H. H. G. (2004). Spatial variability of evaporation and moisture storage in the swamps of the upper Nile studied by remote sensing techniques. *Journal of Hydrology*, 289, 145–164.
- Morse, A., Kramber, W. J., & Allen, R. G. (2003). Preliminary computation evapotranspiration by land cover type using TM data and SEBAL. *Paper presented at International Geoscience and Remote Sensing Symposium, Toulouse, France*.
- Morse, A., Kramber, W. J., & Allen, R. G. (2005). Mapping evapotranspiration from satellites. *Southwest Hydrology*, 18–19 May/June.
- Mu, Q., Heinsch, F. A., Zhao, M. S., & Running, S. W. (2007). Development of a global evapotranspiration algorithm based on MODIS and global meteorology data. *Remote Sensing of Environment*, 111, 519–536.
- Mu, Q., Zhao, M., & Running, S. W. (2011). Improvements to a MODIS global terrestrial evapotranspiration algorithm. *Remote Sensing of Environment*, 115, 1781–1800.
- Mueller, B., et al. (2011). Evaluation of global observations-based evapotranspiration datasets and IPCC AR4 simulations. *Geophysical Research Letters*, 38, L06402 06410.01029/02010GL046230.
- Nagler, P. L., Cleverly, J., Glenn, E., Lamplkin, D., Huete, A., & Wan, Z. (2005). Predicting riparian evapotranspiration from MODIS vegetation indices and meteorological data. *Remote Sensing of Environment*, 94, 17–30.
- NASA-JPL (2008). HyspIRI Whitepaper and workshop report. : JPL Publication 2009.
- Norman, J. M., Anderson, M. C., Kustas, W. P., French, A. N., Mecikalski, J. R., Torn, R. D., et al. (2003). Remote sensing of surface energy fluxes at 10¹-m pixel resolutions. *Water Resources Research*, 39, doi:[10.1029/2002WR001775](https://doi.org/10.1029/2002WR001775).
- Norman, J. M., & Becker, F. (1995). Terminology in thermal infrared remote sensing of natural surfaces. *Remote Sensing Reviews*, 12, 159–173.
- Norman, J. M., Divakarla, M., & Goel, N. S. (1995a). Algorithms for extracting information from remote thermal-IR observations of the earth's surface. *Remote Sensing of Environment*, 51, 157–168.
- Norman, J. M., Kustas, W. P., & Humes, K. S. (1995b). A two-source approach for estimating soil and vegetation energy fluxes from observations of directional radiometric surface temperature. *Agricultural and Forest Meteorology*, 77, 263–293.
- Norman, J. M., Kustas, W. P., Prueger, J. H., & Diak, G. R. (2000). Surface flux estimation using radiometric temperature: A dual temperature difference method to minimize measurement error. *Water Resources Research*, 36, 2263–2274.
- Owens, K. M., & Moore, G. W. (2007). Saltcedar water use: Realistic and unrealistic expectations. *Rangeland Ecology and Management*, 60, 553–557.
- Price, J. C. (1980). The potential of remotely sensed thermal infrared data to infer surface soil moisture and evaporation. *Water Resources Research*, 16, 787–795.
- Price, J. C. (1990). Using spatial context in satellite data to infer regional scale evapotranspiration. *IEEE Transactions on Geoscience and Remote Sensing*, GE-28, 940–948.
- Seneviratne, S. I., Courti, T., Davin, E. L., Hirschi, M., Jaeger, E. B., Lehner, I., et al. (2010). Investigating soil moisture-climate interactions in a changing climate: A review. *Earth-Science Reviews*, 99, 125–161.
- Shafroth, P. B., Brown, C. A., & Merritt, D. M. (2010). Saltcedar and Russian olive control demonstration act science assessment. *U.S. Geological Survey Scientific Investigations Report 2009-5247* 143 pp.
- Su, Z. (2002). The surface energy balance system (SEBS) for estimation of the turbulent heat fluxes. *Hydrology and Earth Sciences*, 6, 85–99.
- Thenkabail, P. S., Hanjra, M. A., Dheeravath, V., & Gumma, M. (2010). Global croplands and their water use from remote sensing and nonremote sensing perspectives. In Q. Weng (Ed.), *Advances in environmental remote sensing: sensors, algorithms and applications* (pp. 383–420). : Taylor and Francis, CRC Press.
- Thenkabail, P. S., Lyon, G. J., Turrall, H., & Biradar, C. M. (2009). *Remote sensing of global croplands for food security*. Boca Raton, FL: CRC Press/Taylor & Francis Group.
- Timmermans, W. J., Kustas, W. P., Anderson, M. C., & French, A. N. (2007). An intercomparison of the surface energy balance algorithm for land (SEBAL) and the two-source energy balance (TSEB) modeling schemes. *Remote Sensing of Environment*, 108, 369–384.
- Tolk, J. A., & Howell, T. A. (2001). Measured and simulated evapotranspiration of grain sorghum grown with full and limited irrigation in three high plains soils. *Transactions of ASAE*, 44, 1553–1558.
- Trezza, R., Allen, R. G., Robison, C. W., Kramber, W. J., Kjaersgaard, J. H., Tasumi, M., et al. (2008). Enhanced resolution of evapotranspiration from Riparian systems and field edges by sharpening the Landsat thermal band. *Paper presented at ASCE-EWRI Environmental and Water Resources Conference, Honolulu, Hawaii*.
- Wetzel, P. J., Atlas, D., & Woodward, R. (1984). Determining soil moisture from geosynchronous satellite infrared data: A feasibility study. *Journal of Climate and Applied Meteorology*, 23, 375–391.
- Zhan, X., Kustas, W. P., & Humes, K. S. (1996). An intercomparison study on models of sensible heat flux over partial canopy surfaces with remotely sensed surface temperatures. *Remote Sensing of Environment*, 58, 242–256.